Cape Peninsula University of Technology

IMPROVEMENT OF A POWER SYSTEM SECURITY BY FAULT CURRENT REDUCTION

by

Mr. Inga Mpontshane

Dissertation submitted in partial fulfilment of the requirements for the degree

Master of Engineering in Energy

in the Department of Electrical, Electronic & Computer Engineering

of the Faculty of Engineering and the Built Environment

at the Cape Peninsula University of Technology

Supervisor: Prof. Atanda Raji

Bellville campus
November 2023

DECLARATION

I, Inga Mpontshane, declare that the contents of this dissertation represent my own unaided work, and that the thesis/dissertation has not previously been submitted for academic examination towards any qualification. Furthermore, it represents my own opinions and not necessarily those of the Cape Peninsula University of Technology.

Signed_____ **Date** 12 November 2023

ABSTRACT

The generation of electricity from Renewable energy sources (RES) (wind, solar, hydro, etc.) has grown at an exponential rate in recent years. This is due to the global energy industry becoming even more mindful of the environmental impact caused by the generation of electricity from fossil fuel energy sources (coal, nuclear, diesel, etc.). Distributed generation and micro-grids are some of the topologies that are employed by many grid designers around the world to work towards achieving a 100% green energy network. Solar and wind energy are the dominating energy sources in the renewable energy industry and grid codes of many countries require fault ride-through capabilities for all inverter-based RES.

Consequently, the bulk integration of renewable energy sources into the conventional power grid significantly compromises the power system's security. The fault current levels increase, and the direction of the power flow changes significantly. This poses a risk of exceeding the fault current rating of the installed power system apparatus and would result in major power system outages or much worse cause devastating damages to the apparatus.

Hence, this dissertation analyses different fault current limiting measures, techniques, and technologies that are used to reduce the intermittent and inevitable fault currents. An extensive literature review is caried out and Resistive Superconducting Fault Current Limiter (rSFCL) is found to be a preferred technology. A MATLAB Simulink model of rSFCL is designed and simulated. The rSFCL model is further integrated into an IEEE 9 bus power system to test its impact on fault current levels at different buses.

Through different simulation scenarios, the results shows that the rSFCL model does indeed reduce the fault current levels. When the rSFCL model is installed in the power system model near the energy source the fault current peak levels are reduced by approximately 27.05 %.

Keywords: Power system, Fault current, renewable energy sources, fault current limiter, superconductor, non-superconductors, MATLAB Simulink.

ACKNOWLEDGEMENTS

I wish to thank:

- My dear wife Mrs Amolathile Mpontshane, for all the support and understanding of the many hours spent when conducting this research. You are truly a life partner I can always count on.
- My family for all the support in everything I do especially my parents Mr Jonguxolo Mpontshane and Mrs Nomonde Mpontshane whom I am always in contact with.
- My Supervisor Prof. Atanda Raji for all the support, guidance, and patience. This would have never been possible without you.
- My colleagues at Eskom, whom we always help and motivate each other.

DEDICATION

I would like to dedicate this research to my younger sisters whom I can observe that they are taking their education very seriously, with the last born even intending to become a doctor in the near future. This is to demonstrate to you ntombi zama-goqolo that through hard work and dedication you can achieve anything.

For (Miss Silindokuhle Mpontshane & Miss Sanelisiwe Mpontshane)

Table of Contents

LIST OF FIGURES

Chapter 1

Chapter 2

Chapter 3

LIST OF TABLES

ABBREVIATIONS AND ACRONYMS

AC	Alternating Current
CER	Conventional Energy Resources
CVS	Controlled Voltage Source
DC	Direct Current
DG	Distributed Generation
DOE	Department of Energy
FCL	Fault Current Limiter
HTS	High-Temperature Superconductors
iSFCL	Inductive fault current limiters
LV	Low Voltage
MATLAB	Matrix Laboratory
PV	Photovoltaic
RES	Renewable Energy Sources
RMS	Root Mean Square
rSFCL	Resistive Superconducting Fault-Current Limiters
SC	Short Circuit
SCC	Short Circuit Current
SFCL	Superconducting Fault-Current Limiters

GLOSSARY

Busbar	A common connection point for different feeders operating at the same voltage level.
Distributed generation	The use of a variety of renewable energy technologies to produce and supply electricity near the load.
Fault current limiter	A device that is used to reduce or limit prospective fault current in an event where a power system disturbance has occurred.
Grid codes	A technical specification that indicates the operating requirements that independent power producers need to meet before they connect to the national grid.
Hybrid	A combination of different technologies to produce power.
Load	A portion of the power system that consumes electric energy.
MATLAB Simulink	A network simulation software that is used to model and simulate different power system networks.
Microgrid	A small-scale electric grid that operates in islanded mode.
Protection system	A system that protects the power system against abnormal conditions such as short circuits.
Quenching state	A state at which the FCL is inserting a very high impedance into the network to reduce SCC.
Short Circuit / Fault	A low resistive path for a current to flow caused by two nodes with different potentials making contact in an electrical network.
Superconducting FCL	A device that can be installed in a strategic position of a power system to limit the inevitable short circuit currents
Superconducting state	A state at which the FCL is inserting a very low impedance into the power system to allow normal load current to flow through without any losses.

CHAPTER 1: Introduction

1.1 Background of the research problem

The penetration of Renewable energy sources (RES) (wind, solar, hydro, etc.) has grown at an exponential rate in recent years with many of them being integrated into the energy distribution network to form Distributed Generation (DG). Solar Photovoltaic (PV), wind farms, and small-scale hydro plants are some of the leading technologies in the green energy industry (Buraimoh & Davidson, 2020). Thus, the high penetration of distributed and renewable energy sources causes an increase in fault current levels in the power system, and the direction of power flow changes significantly (Takele, 2022). Precisely, now that the grid codes of many countries require a fault ride-through capability for all inverter-based RES (Buraimoh & Davidson, 2020). Fig. 1. 1 shows the global change in electricity generation by source from 2019 to 2025 (Anon, 2020). This chart indicates a projection of continuous growth in the generation of electricity from RES. Therefore, the challenge of inevitable increased fault current levels is expected to continue.

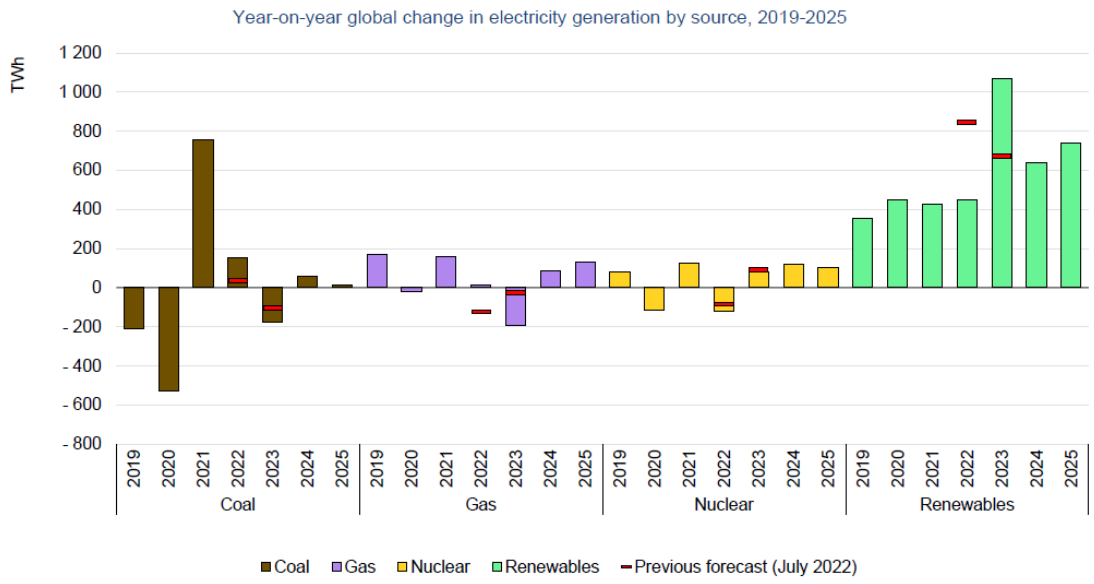

Fig. 1. 1: Global change in electricity generation by source from 2019 to 2025 (Anon, 2020)

These increased fault current levels are intermittent and pose a risk of exceeding the current and voltage threshold of the installed power system apparatus ((Gonçalves Sotelo et al., 2022)(Gabr et al., 2021)(Fang et al., 2023)(Wang et al., 2023)). A traditional solution to this problem would be to replace the existing apparatus with those of higher rating to accommodate the new fault levels or to build parallel circuit(s) to split the fault current as stipulated by Kirchhoff's current law. However, such solutions would result in high financial costs (Gonçalves Sotelo et al., 2022). Hence, Fault current reduction technologies and techniques such as reconfiguring the network, adding series reactors, using fault current

limiters, etc. are some of the technologies that have been popular in recent studies (Gonçalves Sotelo et al., 2022).

1.2 Statement of research problem

The integration of renewable energy sources (RES) (Solar, wind, hydro, etc.) into the conventional power grid has a significant impact on current fault level. The fault currents increase drastically and different ways to reduce them are required to maintain power system stability.

1.3 Aims and Objectives of Research

The following are the aims and objectives of this research:

a) To reduce fault current as a result of incorporation of RES.
b) To build a model to investigate the effect of fault current limiting technology.
c) To propose strategies and techniques for reducing fault currents in a network with integration of RES.

1.4 Research Questions

a) How does the integration of renewable energy sources affect the security of the power system?
b) How do fault ride-through capabilities affect fault current levels?
c) How do fault current reduction technologies improve the power system security?

1.5 Research Design and Methodology

The design and methodology of this research was based on studying the available literature on short circuit currents, its causes, and its source of supply. Furthermore, the literature on different fault current limiting measures and different types of fault current limiters was studied. A prototype of a preferred fault current limiter was built on MATLAB Simulink and different scenarios were simulated. The model consist to variables such as current and temperature.

1.6 Delineation of the research

- The types of RES that this research focused on are solar, wind, and hydro energy because those are the types that have major contribution to the fault levels.
- The testing of the impact of the fault current reduction technology will be done on software only, no practical model will be built.
- Few fault current limiters are commercially available with the majority of them being still under development.

1.7 Research outline

1.7.1 Chapter 1 – Introduction

This chapter provides a general background of this study, the statement of the research, aims and objectives, research design and methodology, delineation of the research, and research outcomes.

1.7.2 Chapter 2 – Literature Review

This chapter covers an in-depth review of the literature that has been published on short circuits (SC) and investigate major contributors of SCC such as distributed energy sources and renewable energy sources. The literature on different strategies/techniques that can be used to reduce/limit SCC was also presented in this section to evaluate the best suitable for different applications. Furthermore, the literature on the classification of FCLs was also covered in this chapter.

FCL was identified to be a chosen technology, thereafter, the literature on FCL, attributes of a good FCL, advantages and disadvantages of FCL, application of FCL, case studies of FCL application, FCL classification, different types of FCL, and control strategies of FCL were explored in detail.

1.7.3 Chapter 3 – Mathematical Modelling and simulation

In this chapter, the mathematical expression of Periodic and Aperiodic components of SCC, SCC on a simplified power system, E – J Characteristics, and determination of shunt resistance was elucidated.

Furthermore, a Modelling and Simulation of rSFCL was performed by making use of MATLAB Simulink. The model was done based on the specific desired outcome which is to have a FCL that has nearly zero impedance during normal operation of the network, and adequately high impedance during a faulty condition. Different scenarios of the rSFCL model were simulated to assess the performance of the model. The rSFCL model was further, integrated to an IEEE 9 bus system to evaluate its effectiveness.

1.7.4 Chapter 4 – results and discussions

In this chapter, the data that was collected during the simulation in chapter 3 was analysed and compared to support all conclusions drawn.

1.7.5 Chapter 5 – Conclusion

In this chapter, the conclusion of this study's general outcomes was elucidated, and recommendations were given. Furthermore, future work of this study was given.

CHAPTER 2: Literature Review

2.1 Introduction

The global energy industry has put most of its efforts towards researching technologies that will give 100% green energy to reduce the negative environmental impact caused by the immensely utilised fossil fuel-based energy resources. The recent trends shows that energy storage is one of the areas that have been attracting more attention as renewable energy is intermittent and not dispatchable. These initiatives are largely supported by energy sectors of many countries with some even working towards set deal lines to achieve green energy.

Even though this initiative is for a good cause, the energy industry tends to turn a blind eye toward the impact that 100% green energy will inevitably have on power system security. Thus, it is vital for efforts to be invested in finding solutions for the challenges that comes along with green energy initiatives to avoid unforeseen grid collapse. Increased levels of SCCs are one of the major challenges that have arisen and it's the area that this study will focus on.

This chapter will cover published literature of short circuits, different strategies/technologies to reduce/limit SCC, classification of Fault Current Limiting Measures, and broader view on fault current limiters.

2.2 Short Circuits (SCs)

Short Circuit (SCs) are the most common abnormality that occurs in an operational power system and they can be defined as a low resistive path for a current to flow caused by two nodes with different potentials making contact in an electrical network. (Safaei et al., 2020a).

2.2.1 Causes of SCs

SCs are caused by the occurrence of abnormal events such as (Chetty, 2016):

a) Breakdown of the insulating medium
b) Lightning strike
c) Huge bird streamers
d) Trees growing into power lines
e) Corrosion
f) Cane fires
g) Mechanical failure of the equipment

Such events lead to an unwanted connection/s of parts of a circuit/s. These can be characterised by extremely high currents at a particular point for a short period usually milliseconds, until interruption takes place by the protection system (Chetty, 2016).

2.2.2 Types of Short Circuits

SCs are divided into two groups, namely symmetrical (balanced) and asymmetrical (unbalanced) SCs (Mutambudzi & Raji, 2020).

Symmetrical SCs usually have a high magnitude when compared to asymmetrical SCs. The following are the most common faults that occurs in the network:

Symmetrical Short Circuits

- Three Phase – Earth

Asymmetrical Short Circuits

- Single phase – Earth
- Phase – Phase
- Phase – Phase – Earth
- Phase – Phase – Phase
- Sensitive short circuit

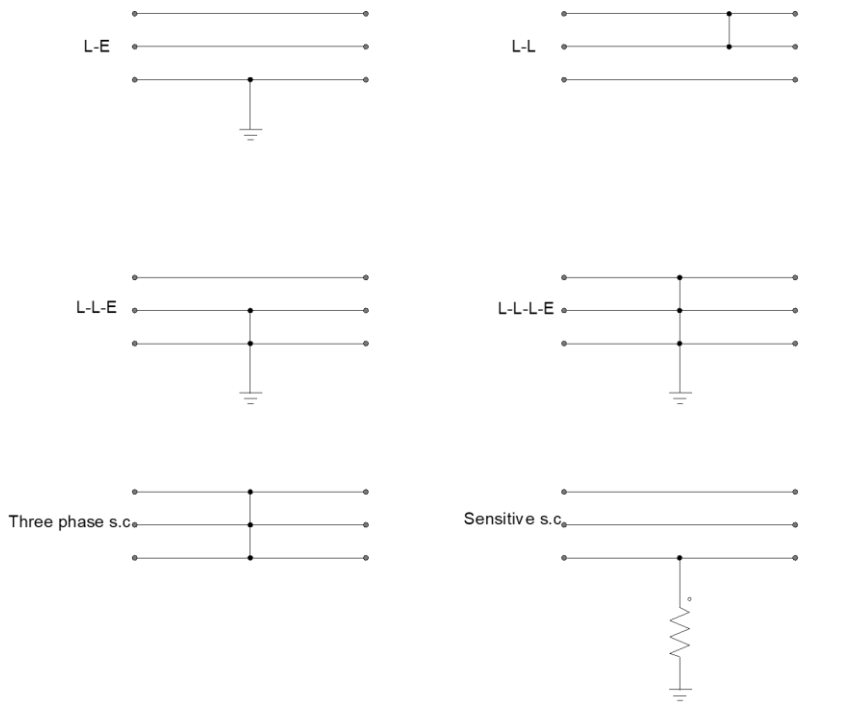

Fig. 2. 1: Different types of power system faults (Chetty, 2016)

When a short circuit occurs near a generator, it increases to an extremely large value and then gradually decreases through three different stages namely, Sub transient, transient,

and steady-state as demonstrated in Fig. 2. 2 (Manditereza, 2019). The gradual decrease is caused by the variation in the impedance of the generator, in this case the dominant impedance, it damps the SCC (Gers & Holmes, 2021). Sub transient state lasts for 10 – 20 ms, the transient state lasts for 500 ms, and the steady state lasts for the rest of the fault duration until it's interrupted by the protection devices.

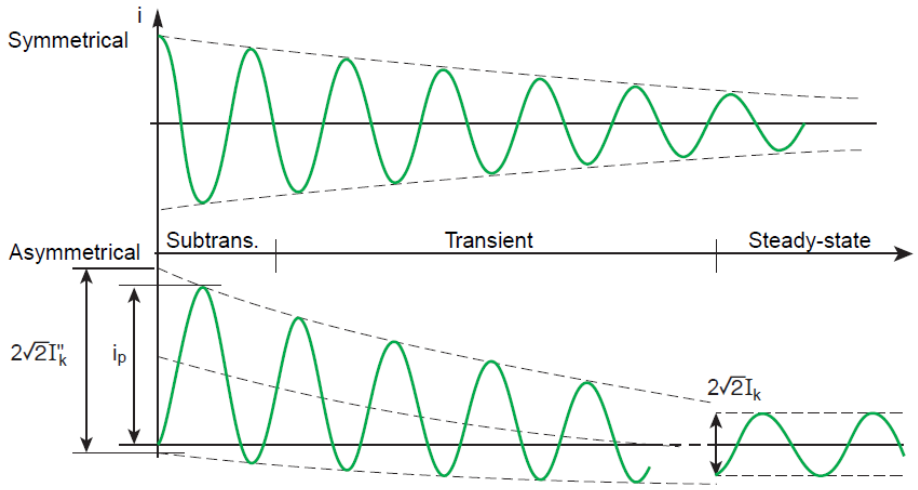

Fig. 2. 2: Symmetrical and asymmetrical SCC near a generator(Gers & Holmes, 2021)

2.2.3 Effects of SCCs

When a Short Circuit occurs, the current can increase to more than 10 times the full load current causing dynamic thermal stress to the installed grid apparatus such as generators, conductors, and circuit breakers (CB) (Safaei et al., 2020a). This phenomenon can have a devastating impact on nearby personnel, and in most cases the continuity of electricity supply gets interrupted (Chetty, 2016). Power outages consequently cause a ripple effect to the economy with ordinary people being affected the most.

The following are the general effects of SCCs on the power system (Safaei et al., 2020a):

a) Causes voltage swells and voltage sag in busbars that do not have a fault.
b) Causes negative impact on the economy and increase in unsupplied energy.
c) Compromise of power system stability and power system quality index.
d) Causes the Mechanical oscillations on the generator and motor's shaft to dampen.
e) Causes stress on the damping windings of synchronous machines and opposite rotational inertia.
f) Reduces the torque in induction motors.
g) Causes voltage sags in buses that are voltage sensitive.
h) Electromagnetic interference.
i) Corrosion in the connection area.

j) Causes an increase in the demand of reactive by transmission lines and power transformers.

2.2.4 Protection against SCC

Power system protection devices such as Switch gears (SG), Current transformers (CT), Voltage Transformers (VT), Intelligent Electronic Devices IEDs, etc. are used to protect the power system against SCC. Fault analysis is carried out to determine the magnitude of SCCs flowing in the network. This information is essential in the grading of protection systems and choosing equipment with appropriate ratings. In complex networks fault analysis is carried out using power system packages and simulation software such as Power factory Dig Silent and MATLAB Simulink.

The magnitude of SCC can be calculated based on the amount of power supplied (MVA) by the energy sources, the voltage (V) rating of the network, and the impedance (Z) of the network. Alternatively, the SCC magnitude can be measured on respective busbars with current and voltage transformers.

2.3 Source of SCC

2.3.1 Distributed Energy Sources

Distributed energy sources, referred to as Distributed Generation (DG) can be defined as the use of a variety of renewable energy technologies to produce and supply electricity near the load. In some cases, DG is a combination of RES and Conventional Energy Resources (CER). Fig. 2. 3 is a demonstration of a typical DG power grid that consists of fossil fuel-based energy sources and renewable energy sources. This diagram demonstrates the level in the network where each energy source is connected. CER are connected in the transmission system and RES are connected in the Distribution system.

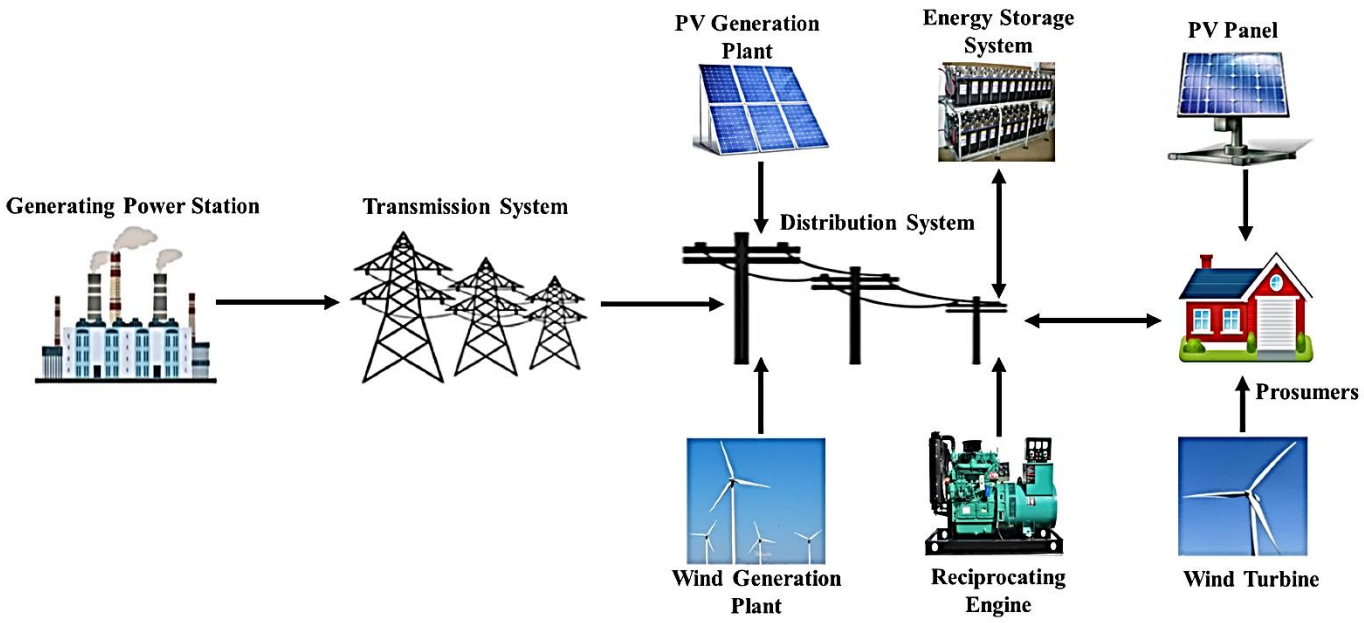

Fig. 2. 3: Micro grid (Salam et al. 2023)

2.3.1.1 Benefits of DG (Sohail et al. 2022):

- Improvement of voltage profile.
- Reduction of power loses.
- Unloading sub-transmission and transmission system.
- Enhancing power quality and reliability.

2.3.1.2 Drawbacks of DG (Adnan et al., 2018):

- Increasing the Short Circuit Currents (SCC).
- Causes harmonic interference.
- Steady voltage drops.
- Grid voltage rise.
- Frequency instability due to intermittent energy generation

2.3.1.3 SCCs contribution of DG

The theory behind the significant increase in SCC can be explained using a superposition principle where every current source that is integrated into the grid contributes an additional amount of current towards the SCC of the network (Sohail et al., 2022). Most of the distributed generators are integrated in the distribution system as shown in Fig. 2. 3. And most short circuits occur in the Distribution system. Thus, the distributed generators subsequently directly contribute to the high fault current levels as they increase the number of current sources in the network and they are located very close to where short circuits usually occur (Sohail et al., 2022).

2.3.2 Renewable Energy Sources (RES)

A substantial amount of literature indicates that the high penetration of RES is one of the leading sources of increased fault current levels in the power system (Gonçalves Sotelo et al., 2022)(Gabr et al., 2021)(Fang et al., 2023)(Wang et al., 2023). The increase factor can be influenced by several factors i.e. the level of penetration of RES in the industry (Sule, 2022), whether the renewable energy sources are inverter-based or non-inverter-based, the location on the system where the fault has occurred, and many more factors (Takele, 2022).

(Safaei et al., 2020a) states that synchronous generators generally have a major SCC contribution under steady state condition. However, large induction motors have a dominate effect on increasing the transient component of SCC. (Safaei et al., 2020a) also indicates that DGs SCC contribution depend on the type of RES used. For example, the SCC contribution of the inverter-based RES like Photovoltaic (PV) has a contribution of approximately 1.2 times the nominal current and doubly fed induction generator (DFIG)-based wind turbines has a SCC contribution of about 6 times the rated current.

2.3.2.1 Photovoltaic (PV)

Fig. 2. 4: Photovoltaic Plant (Anon, 2020)

According to research done by a German physicist, Albert Einstein, a deep nuclear fusion reaction occurs in the core of the sun and photons are released and they travel a very long distance to reach earth and other planets in the solar system. When these photos reach earth, some elements or material that are on earth can absorb them and react by releasing electrons. This phenomenon is called photoelectric effect and it is the main concept that is used on Photovoltaic technology.

The basic principle of operation for photovoltaic plant is that it converts energy from solar radiation to electrical energy by making use of solar panels. The popular material that is

used to make solar panels by most panel manufactures are silicon (Si) and gallium arsenide semiconductor material (Meisen, 2014). When these two semiconductors are put in contact with each other to form a solar panel and expose to radiant sunlight, electrons are released to enable the flow of electric current between them (Meisen, 2014). The rate at which electricity is produced is determined by the intensity of the sunlight (Gumilar et al., 2020). Solar radiation is dependent on following three factors (Meisen, 2014):

- Direct radiation which reaches the earth directly
- Diffuse radiation which reaches the earth through scattered radiation that are caused by atmospheric particles
- Albedo sunlight that are the light reflected from the surface or objects

Photovoltaic systems are made of structures that have several components such as:

- Photovoltaic panels
- Inverter
- Electrical connections
- Fixed mechanical structure
- Energy storage system

The mechanical structure must be strategically positioned to capture as much sunlight throughout the day. One of the modern ways to optimise the exposure of the solar panel to the sunlight is to have a mobile mechanical structure that is controlled by a sensor that will make the structure to follow the sun throughout the day.

The production of power from PV plants has several advantages such as, no emission of toxic gasses to the atmosphere, low maintenance as it has no moving parts, and available anywhere across the world (Meisen, 2014). However, some disadvantage also exists such as its intermittent nature since its climate dependant and can only produce energy during the day.

Energy storage technologies such as, battery, flywheel, and hydro plants are used to store electricity that is generated by the PV plant to make it available during the time the sunlight is not available. Inverters are also one of the major components as they convert the produced DC power to AC power that is usable by consumers.

2.3.2.2 Wind farms

Fig. 2. 5: Wind farm (Anon, 2020)

This type of Wind energy is one of the profound renewable energy sources that are indirectly produced by solar radiation, the solar radiation heats up the earth surface and cause different pressure of air. The hot air rise and then cool air gets absorbed by the surface. This interchange of air is what causes wind. Mankind have used wind energy for different purposes such as pumping water, powering sawmills, and most recently producing electricity.

The principle of operation for this type of power plant is that it utilizes natural wind to rotate turbines that are connected to a generator shaft. when the wind blows it exerts a turning force on the blades of a wind turbine. The rotating blades turn the shaft that is connected to the gearbox. The gearbox increases the rotational speed of the shaft. The shaft is connected to electricity generator, which uses magnetic field to convert the rotation to electrical energy. There are different types of wind turbines and the most popular one is the horizontal axis wind turbine.

The following are factors that influence the energy produced by wind farms (Gumilar et al., 2020) :

- Speed at which the wind blows.
- The diameter of the wind turbines.
- The number blades of blades that the turbine has.

The efficiency of the blades are calculated based on the following formulas:

$$E = W = F_s \qquad (2.1)$$

$$F = ma \quad (2.2)$$

$$F = mas \quad (2.3)$$

$$P = \frac{1}{2}mv^2 \quad (2.4)$$

$$P = \frac{1}{2}pAv^3C_p \quad (2.5)$$

Where:

E : Kinetic Energy

P : Power

m : Mass

t : time

v : Wind Speed

Studies shows that wind energy is the second largest form of RES after hydro power-plant, and it is expected to be the largest source of energy by year 2050 with a projected capacity of 8000 GW across the globe. The constant growth in wind turbine technology such as double fed induction generators has enabled the price of kWh to drop by approximately 35% for both offshore and onshore wind generators between the year 2010-2019 (Demin et al., 2023).

The following are the advantages of wind energy:

- Produces clean energy
- It's a sustainable source
- It generates electricity cheaper than the fossil fuels
- Its environmentally friendly

The average working life span of a wind turbine is 20-25 years and there after it must be replaced by a new one. From the early 1980's up until now, the price of electricity generated from wind worldwide has dropped by more than 80%

2.3.2.3 Fault current contribution of Photovoltaic (PV) and Wind energy

Photovoltaic (PV) and wind energy are the two mostly used RES in the energy industry around the world and this is due to its abundance in many geographic locations (Buraimoh & Davidson, 2020). Among many, One of the common attributes of these two energy sources is that they are inverter based energy sources (Liu et al., 2019)(Buraimoh & Davidson, 2020). Which means that power electronics devices are used to convert the produced DC power to AC power that is generally flowing in the grid. In the past, these inverter-based energy sources were afforded exemption by the grid codes to disconnect during fault condition to protect them from system abnormalities (Buraimoh & Davidson,

2020). This exemption was done because the energy supply from RES was of small margin compared to the energy supplied by conventional energy sources (Buraimoh & Davidson, 2020). However, with the recent high penetration of RES, grid codes of many countries require fault current ride through (FCRT) capabilities from all solar and wind farms in order to maintain power system stability (Buraimoh & Davidson, 2020). Consequently, FCRT capabilities of RES present challenge of inevitable increased fault currents.

2.3.2.4 Fault current ride through

Many countries around the world with growing penetration of RES have introduced amendments to their grid codes that are concentrated on the integration of Photovoltaic and wind farms into the grid. These inverter-based energy sources are required to have a fault ride-through capability to ensure the stability of the power system during fault conditions (Buraimoh & Davidson, 2020) (Wan et al., 2022). According to (Liu et al., 2019) the amendment of grid codes which demands fault ride-through capabilities comes along with increased fault current levels. Subsequently, the high fault current levels present an inevitable challenge of encroaching on the rated current ratings of installed apparatus and protection devices (Liu et al., 2019). According to (Fang et al., 2023) technics like grid and bus splitting, series reactors, and/or high short circuit impedance transformers are usually used to limit the short circuit currents. However, these technics have a significant impact on the power system stability and reliability (Fang et al., 2023).

2.3.2.5 Hydro power

Fig. 2. 6: Hydro power dam (Anon, 2012)

Hydro power is also considered as one of the profound RES that are indirectly produced by solar radiation. When solar radiation heats up the earth surface, a cycle of evaporation and rainfall occurs which then result into water flowing through rivers and filling up dams

(Anon, 2012). Hydro-electric engineering therefor make use of the water deposited at a suitable head to drive generator turbines. An essential requirement is that the water should be located at an elevated position where they can be discharge and flow to a lower reference point. When the water is discharged, potential energy is created and is therefore used to drive the turbines that are connected to the generator shaft (Anon, 2012).

The International Energy Agency's (IEA's) (World Energy Outlook 2013) states that, energy produced from hydro power across the globe is expected to increase from 3490 GWh in 2011 to approximately 5500 and 5900 GWh by 2035, and that will account for 15% of total global electricity generation.

Hydro power plants can also be used as energy storage facilities. In such a system, two dams will be involved, one situated at an elevated position and another one at a lower level. During peak hours of the load, where maximum power demand is reached, the water on the elevated dam will be discharged and electricity will be supplied to the grid. When the demand of electricity has dropped, the unused electricity in the grid will be used to pump the water from the lower dam to the elevated dam and wait to be discharged again during peak demand.

2.3.2.6 Small-scale Hydro power and Small-scale Wind farms SCC contribution

The small-scale hydro power and small-scale wind farms are some of the renewable energy technologies that are used in DG which are non-inverter based. The non-inverter based renewable energy technologies utilize rotating machines like synchronous generator (small scale hydro power) and induction generators (small scale wind farm) (Masaud & Mistry, 2017).

Synchronous generators has a higher fault current contribution compared to induction generators and inverter based RES (Masaud & Mistry, 2017). And this is due to its design configuration of field current being supplied from external DC source and the prime mover drives the rotor to supply the required voltage in stator winding (Masaud & Mistry, 2017). Subsequently, a continues fault current is injected into the system when a system abnormality occurs. When a three phase fault occurs in the system, the synchronous generators will inject a sub-transient current of about 6 x rate current for 4 to 6 cycles before it drops down between 400% to 200% of the full load current (Masaud & Mistry, 2017).

When a similar fault occurs near an induction machine, the fault current contribution is initially six times the full load current and then gradually decrease to zero (Masaud & Mistry, 2017). Fault current in induction machines is produced by the presence of field flux

which is generated by the induction from the stator and the field excitation is not kept constant hence the fault current does not remain at steady state (Masaud & Mistry, 2017).

2.4 Different strategies/technologies to reduce/limit SCC

2.4.1 Current Limiting Reactors

According to (Alam et al., 2018) the current limiting reactors are used in power systems to mitigate the impact of SCC and avoid the damage of key power system equipment due to excessive fault currents. However, current limiting reactors have a high impedance during normal operation of the power system. Therefore, the application of FCLs is a promising solution to improve the power system security.

2.4.2 Replace apparatus or reconfigure network

(Tambunan et al., 2019) suggests that the conventional methods that can be used to mitigate high SCC are the replacement of protection devices (Circuit breakers, Current and voltage transformers, etc), use of high impedance transformers, reconfiguration of the power system to split the current, or to apply high voltage level on the system. However, these strategies have an overwhelming disadvantage of high financial cost and high-power losses during normal operation. Henceforth, (Tambunan et al., 2019) agrees with (Alam et al., 2018) that FCLs are an emerging technology that can better solve the problem of increased SCC due to its advantage of low impedance during normal condition and high impedance during fault condition.

(Safaei et al., 2020a) state that the most direct and easy strategy to accommodate the increased fault current levels is to replace the installed power apparatus with those of higher rating. However, a major setback of this approach is that it is very expensive, and it requires a large capital investment.

2.4.3 Disconnect DGs during SC

(Safaei et al., 2020a) suggest that the primary solution to reduce increased SCC is to disconnect the DGs when a fault condition occurs. The advantage of this technique is that the fault levels of the system will remain within acceptable margins and the protection settings would remain the same (Safaei et al., 2020a).

However, the disconnection of DGs during fault condition has an impact on the voltage stability and power quality of the system and for that reason grid codes of many countries require DGs to remain connected to the system even during fault condition (Safaei et al., 2020a).

2.4.4 Adaptive protection scheme

(Safaei et al., 2020a) also indicates that adaptive protection scheme that make use of artificial intelligence concept can be used. However, these schemes make use of complex algorithms that consume a lot of time, not economically feasible, and often require pre-defined data of system for different conditions (Safaei et al., 2020a).

2.4.5 Multi-agent-based algorithms

(Safaei et al., 2020a) further, indicates that the multi-agent-based algorithms have been introduced as a solution. However, the multi-agent based algorithms are heavily dependent on communication links and the moment the communication is lost, their operation will be disabled (Safaei et al., 2020a).

2.4.6 Fault Current Limiting Measures

Therefore, the ultimate solution that (Safaei et al., 2020a) propose is the fault current limiting measures and devices which can be used in both transmission and distribution network as suggested by both (Alam et al., 2018) and (Tambunan et al., 2019).

2.5 Classification of Fault Current Limiting Measures

According to (Safaei et al., 2020a) Fault current limiting measures (FCLM) can be classified into two groups, namely topology based measures and equipment based measures as illustrated in Fig. 2. 7.

The **topology-based measures** are those FCLM that do not add any additional equipment into the network but rather changes the configuration of the network to create high impedance paths such as, dividing the network into subsections, breaking the buses into multiple sections, transferring to high voltage levels, ect.(Safaei et al., 2020a).

The **equipment-based measures** are those FCLM that add additional equipment into the power system to create high impedance that will limit the SCC such as, installing transformers with high impedance, installing FCL reactors, high voltage current limiter fuses, ABB-Is-Limiters, fault current limiters, etc, (Safaei et al., 2020a).

(Safaei et al., 2020a) further classifies the FCLM into **passive** and **active** measures. Where passive measures are the traditional approaches that remains on the system even when there are no SCC. And active measures are the new approaches that only connect the FCL device into the network only when there are SCC flowing.

Fault current limiters(FCLs) are a preferred FCLM due to its capability to operate at a very low impedance during a normal operation and high impedance when a SCC occurs (Safaei et al., 2020b).

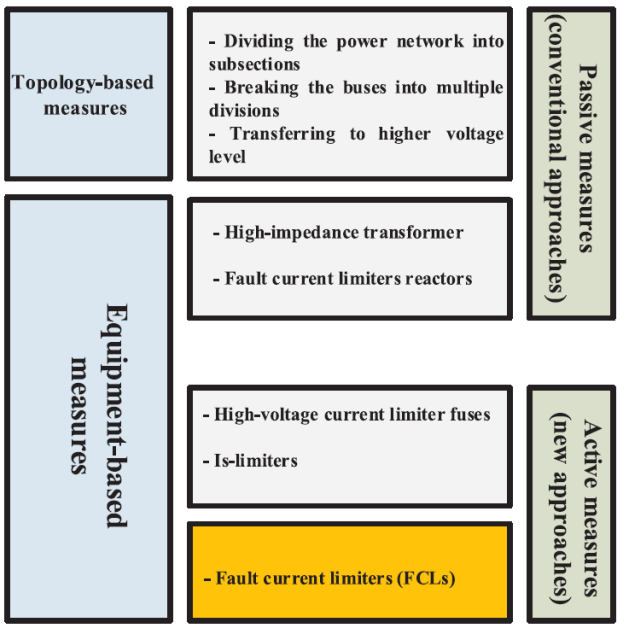

Fig. 2. 7: Classification of fault current limiting measures by (Safaei et al., 2020a).

2.6 Fault current limiters

A FCL can be defined as a device that is used to reduce or limit prospective fault current in an event where a power system disturbance has occurred. Fig. 2. 8 and Fig. 2. 9 demonstrate a microgrid that has a FCL connected in series with a transmission line. Under normal operation, the FCL has a low impedance and allows nominal current to flow through and when a short circuit occurs downstream, the variable impedance on the FCL is increased to block the high fault currents (Gonçalves Sotelo et al., 2022).

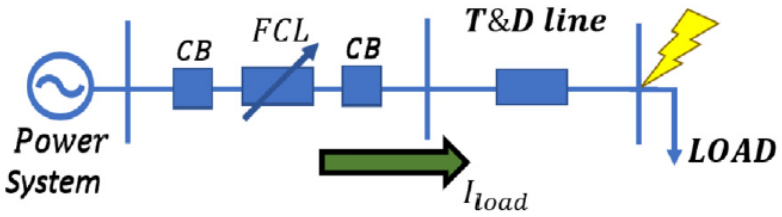

Fig. 2. 8: Micro-grid with FCL connected in series (Gonçalves Sotelo et al., 2022)

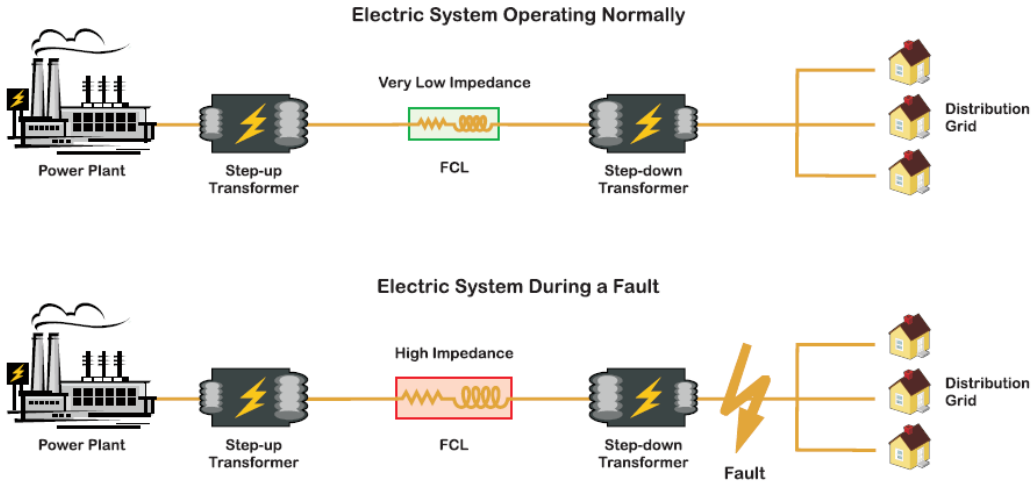

Fig. 2. 9: FCL impedance under normal operation and when a fault occurs (Office of Electricity Delivery and Energy Reliability, 2009)

2.6.1 Attributes of a good FCL (Gonçalves Sotelo et al., 2022).

There are different factors that needs to be considered when choosing a good FCL such as, its environmentally friendliness, variable impedance that can operate at lowest value during normal operation and can dispatch under fault condition, robustness, reliability, operating speed, and capability to coordinate with grid intelligent electronic devices (IED).

2.6.2 Advantages and Disadvantages of FCL (Safaei et al., 2020a)

The literature indicates that there are substantial benefits of using FCL to reduce excessive SCC, however, there are drawbacks that also exist. Table 1 illustrated detailed advantages and disadvantages of using FCLs as a method of reducing SCC.

Table 1: advantages and disadvantages of FCL

Advantages	Disadvantages
• The power system equipment can be designed with lower SCC rating to reduce costs. • During steady state, they do not impose a considerable amount of voltage rise or inject harmonics into the network. • The FCL do not require to be replace after operation. • During steady state, they do not impose a considerable amount of voltage rise or inject harmonics into the network.	• The cost of initial investment is very high, especially the superconducting type FCL. • Relatively high failure rate especially for solid state FCL. • Some have longer recovery time (especially, for the SFCLs). • Requires fault detection algorithms to trigger operation. • False operation in some instances.

• They protect sensitive power system apparatus against exposure to thermal stress caused by high SCC. • No voltage dips or energy losses during normal operation of the circuit. • They take short time to be available for successive fault due to its fast recovery time. • Improves voltage stability. • Cost of upgrading the network can be avoided. • Improves the transient stability of the power system. • Improves voltage stability. • Enhance the stability of induction motors during a short circuit. • Reduce reactive power demanded during a short circuit. • They take short time to be available for successive fault due to its fast recovery time.	

2.6.3 Attributes to be considered in different functional disciplines

There are many different types of FCLs that are produced by different manufactures. Therefore, at times it becomes a challenge to select an appropriate FCL for specific application. Table 2 illustrate the different functional disciplines and FCL attributes to be considered when choosing a good FCL.

Table 2: Disciplines and considered attributes when choosing a good FCL

Disciplines	FCL attributes
❖ Technology	❖ Impedance in normal operation ❖ Impedance when short circuit occur ❖ Quenching time ❖ Recovery time ❖ Level of maturity
❖ Engineering	❖ Installation/Construction process ❖ Required critical components ❖ Required protection system ❖ Voltage and current ratings ❖ Levels of voltage drops

	❖ Required triggers ❖ Power losses
❖ Economic	❖ All costs involved ❖ Required additional equipment ❖ Required cooling system ❖ Availability for purchase ❖ Estimated lifespan ❖ Operation and maintenance ❖ Size and weight
❖ Impact	❖ Environmental impact ❖ Power network impact

2.6.4 Application of FCL

2.6.4.1 System application

(Alam et al., 2018) states that FCLs can be applied in deferent parts of the electric network such as Distributed generation, Generation network, Distribution network, Transmission network, Ac/dc network, and Integrated renewable power generation.

Both superconductive FCLs and Non-superconductive FCLs have been extensively applied in these parts of the power system for varying purposes such as improvement of voltage stability, improvement of fault current ride through capabilities, and protection improvement (Alam et al., 2018). Refer to Fig. 2. 10 for a layout that demonstrate different applications of FCLs.

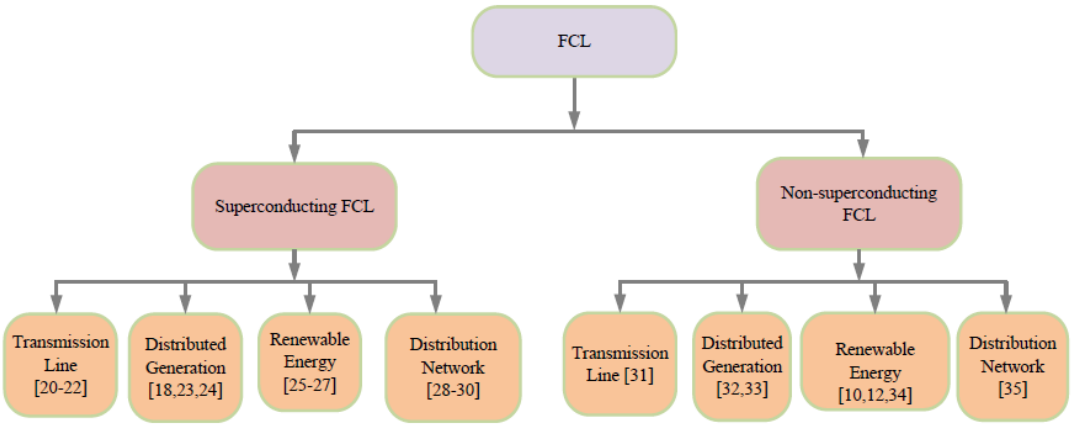

Fig. 2. 10: Application of Superconductive and Non-Superconductive FCLs (Alam et al., 2018)

2.6.4.2 Network application

According to **(Tambunan et al., 2019)** FCL can be strategically placed or installed near the energy sources, between bus bars, and in the distribution network as illustrated in Fig. 2. 11. FCL 1, 2 and 6 are installed near the generators to limit the high SCC contribution

from large generation power plants. Depending on the SCC rating of the transformer the FCL can be installed on the primary winding or on the secondary winding of the transformer. If the transformer can withstand the SCC from the generator, the FCL can be installed on the secondary winding. However, if the transformer cannot withstand the SCC from the generator, the FCL must be installed on the primary winding of the transformer. FCL 4, 5, and 10 are connected to the inter bus connection with 4 used to protect SCC on inter buses and 5 and 10 used to protect SCC on split bus bar (Tambunan et al., 2019). FCL 3, 7, 8, 9, and 11 are connected to protect against SCC on the transmission and distribution feeders.

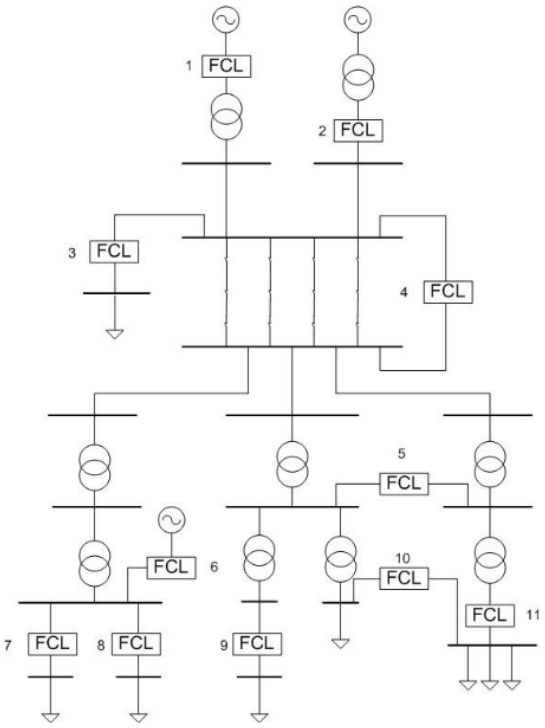

Fig. 2. 11: Strategic locations of FCL by (Tambunan et al., 2019)

Furthermore, fault current limiters can also be used to manage transient fault currents such as inrush currents during a cold load pick up and starting currents of induction generators (Safaei et al., 2020a).

2.6.5 FCLs Case studies

2.6.5.1 Java Bali power system

(Tambunan et al., 2019) presents a case of Java Bali electric network which is the largest electric network in Indonesia. Due to high energy demand, Java Bali has ramped up its energy generation capacity to approximately 28.725,53 MW. Subsequently, the fault currents in 2017 have raised up to more than 50 kA in different regions and they are expected to continue to rise proportional to the growth of the generation capacity as demonstrated in Fig. 2. 12.

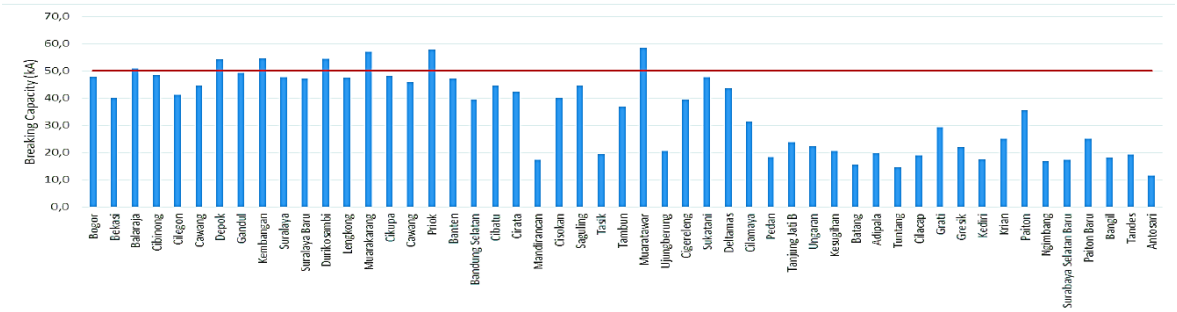

Fig. 2. 12: SCC of java bali in 2017 (Tambunan et al., 2019)

(Tambunan et al., 2019) further outlines a comprehensive framework to be used by PLN which is a state electricity company in Java Bali to mitigate the SCC. In this Framework, the analytic network process (ANP) was used to determine the suitable FCL technology.

Seven FCL technologies were considered, namely air core reactors (ACR), inductive superconducting fault current limiters (ISFCL), iron core reactors (ICR), saturable core fault current limiters (SCFCL), resistive superconducting fault current limiters (RSFCL), and pyrotechnic current limiters (PCL) (Tambunan et al., 2019).

The PCLs were then systematically identified as a preferred FCL technology, and the other six as alternative solutions based on voltage levels to be applied to.

2.6.5.2 South Korea power system

(Alam et al., 2018) states that in **South Korea**, most of the energy generation plants are situated in the northern region and majority of the load is situated in the southern region due to social and environmental constraints. Subsequently, more generators are added in the existing sites and that causes more SCC and instability in the power system (Alam et al., 2018). A hybrid type superconducting fault current limiters (SFCL) was installed to solve these problems (Alam et al., 2018).

2.6.5.3 South Africa Eskom power system

(Chetty et al., 2021) and (Chetty, 2016) present a network study and mitigation measures for increased fault current levels on a 132 kV eThekwini electricity network which is located in South Africa, eThekwini municipality. This study indicates that the increase in fault current levels in this network is due to Eskom increasing its generation capacity to accommodate the growing electricity demand in South Africa.

Eskom is a state owned company that generates, transmits, and distribute majority of South African electricity with an installed maximum capacity of 49191 MW in 2023 (Anon, 2023). Throughout the years most of Eskom's generation capacity have been located in Mpumalanga province where most coal mines are situated (Chetty et al., 2021). With the country shifting to green energy resources and renewable energy procuring approximately

6400 MW, the generation capacity is seemed to be spreading across the country (Chetty et al., 2021). Hence, the challenge of increased fault currents arises.

This study suggests the active and passive methods of reducing the fault currents which involves reconfiguration of the network or adding additional impedance. These measures have been thoroughly explained in (Safaei et al., 2020a).

2.6.6 FCL Classification

2.6.6.1 FCL classification by (Tambunan et al., 2019)

According to (Tambunan et al., 2019) FCL can be classified based as demonstrated in Fig. 2. 13. This paper presented inclusive framework for PLN to reduce invertible SCC in Java Bali electric network. All these FCL were studied into detail and pyrotechnic current limiters (PCL) was systematically identified as a preferred technology for this application.

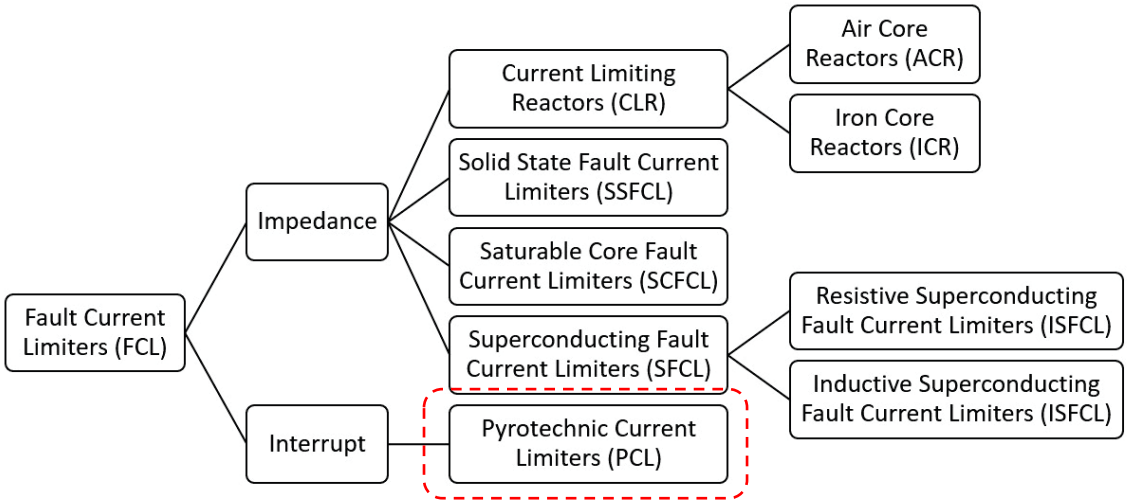

Fig. 2. 13: Classification of FCL according to (Tambunan et al., 2019)

2.6.6.2 FCL classification by (Gonçalves Sotelo et al., 2022)

According to (Gonçalves Sotelo et al., 2022) FCL has been under research and development since the 70s and there are several types with some already commercially available and some still under development. Fig. 2. 14 demonstrate the different types of FCL as classified by this study. Saturated iron core FCL and resistive superconducting FCL are the two most favourable FCLs with fewer disadvantages (Gonçalves Sotelo et al., 2022).

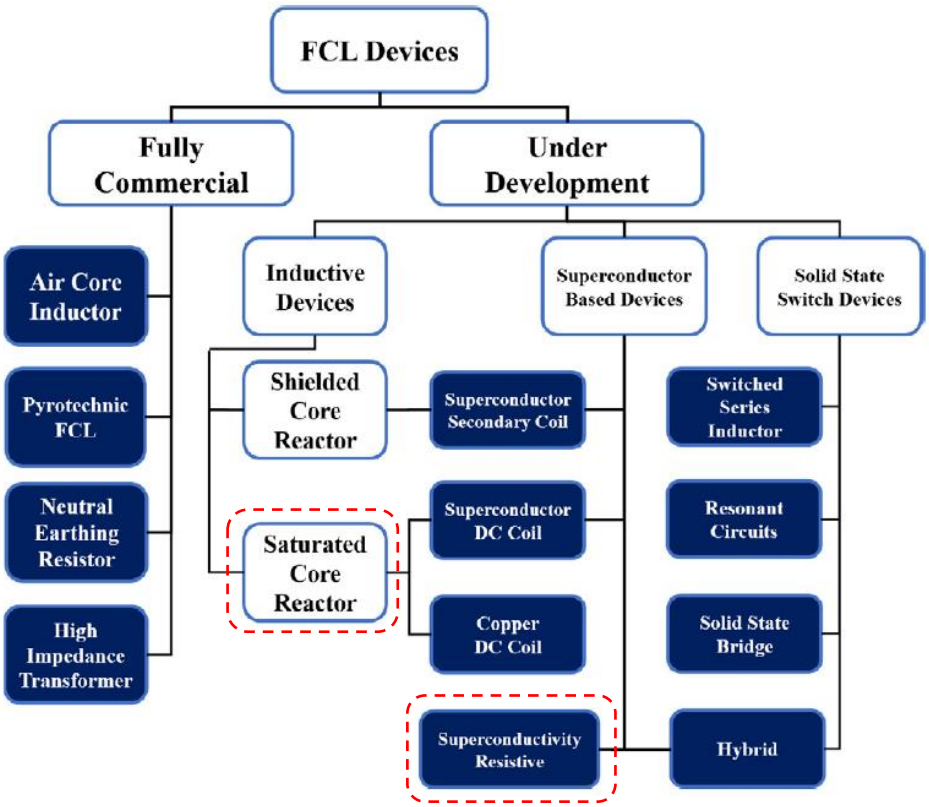

Fig. 2. 14: Different types of FCL(Gonçalves Sotelo et al., 2022)

2.6.6.3 FCL classification by (Safaei et al., 2020a)

According to (Safaei et al., 2020a), fault current limiters technology is divided into four different groups namely: Solid-state fault current limiters, Superconducting fault current limiters, hybrid fault current limiters, and other technologies. Based on the comparative study that was done by (Safaei et al., 2020a) among the four-fault limiter groups, the solid-state fault current limiter is the most preferred one for the power system. This choice was done based on its low costs, flexible structure, and fast advancement in semiconductor science. Fig. 2. 15 illustrate a layout of the above mentioned FCL groups with a breakdown of different technologies that belong to each group.

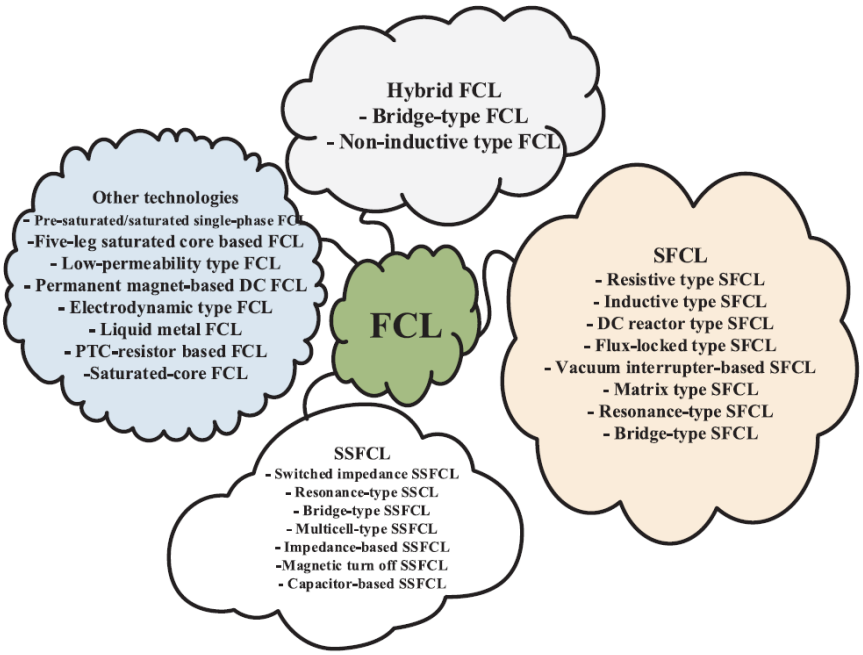

Fig. 2. 15: Breakdown structure of four FCLs groups (Safaei et al., 2020a)

2.6.6.4 FCL classification by (Alam et al., 2018)

(Alam et al. 2018), Classifies FCL into two main groups namely, Superconductive FCLs and Non-Superconductive FCLs. These two groups are further broken-down, and the study lean towards superconductive FCLs as preferred technology. Table 3 illustrate the different FCL types under each group. This literature argues that there are still challenges that restrict the application of FCLs which needs to be addressed such as minimizing interference with adjacent communication lines, coordinated control design between FCL and other protection devices, minimizing losses under normal operation, ability to design optimal parameters, feasibility analysis, and field test in real grid operation.

Table 3: Classification of fault current limiters according to (Alam et al., 2018)

Superconductive FCLs	Non-Superconductive FCLs
❖ Flux-Lock Type SFCL	❖ Bridge Type Fault Current Limiter (BFCL)
❖ Hybrid SFCL	❖ DC Link Fault Current Limiter (DLFCL)
❖ Inductive Type SFCL	❖ Modified Bridge Type Fault Current Limiter (MBFCL)
❖ Magnetic Shield Type SFCL	
❖ Non-Inductive Type SFCL	❖ Series Dynamic Braking Resistor (SDBR)
❖ Transformer Type SFCL	❖ Transformer Coupled BFCL

2.6.6.5 FCL classification by (Patil & Thorat, 2017)

According to (Patil & Thorat, 2017) FCLs can be classified as show in Fig. 2. 16. This literature argues that for application that requires external triggering, the solid state FCL is mostly the preferred choice, and it doesn't require any special cooling systems. For low voltage applications Resistive FCL are better suited. For applications that requires less time of reset perspective the solid state FCL and Hybrid FCL are the preferred choice.

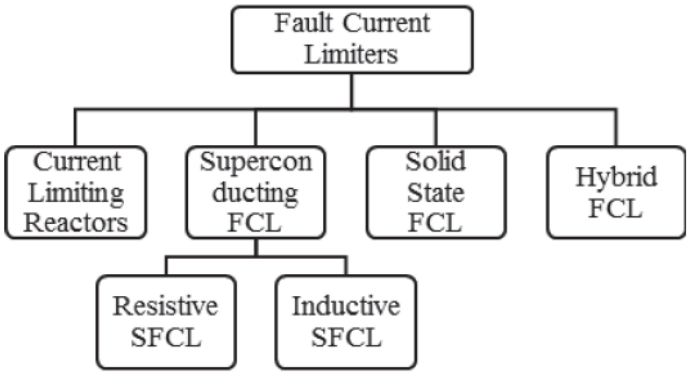

Fig. 2. 16: Classification of FCL by (Patil & Thorat, 2017)

2.6.7 Different types of FCL

2.6.7.1 Current Limiting Reactors (CLR)

A Current Limiting Reactors (CLR) is a series connected reactance that is used to change the impedance of the power system and they are connected between the neutral of the transformers and generators to limit the earth current (Razzaghi & Niayesh, 2011). CLR are divided into two main groups: Dry air core reactors (ACR) and iron core reactors (ICR).

a) Dry Air Core Reactors (ACR)

Dry air core reactors (ACR) consist of one or more concentric cylindrical winding and it is one of the ideal devices to increase the impedance of the system during a fault (Tambunan et al., 2019). However, it has drawbacks such as a voltage drop which requires voltage regulation to compensate for the voltage sag, high stray magnetic field which produce eddy current losses in nearby apparatus, and produce high levels of heat (Asghar, 2018).

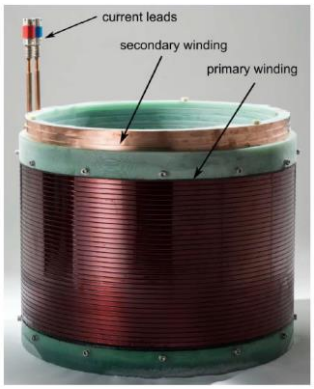

Fig. 2. 17: Dry air core reactors (Tambunan et al., 2019)

b) Iron core reactors (ICR)

The Iron core reactors (ICR) are constructed with core material that have a high magnetic permeability compared to air core reactors (Tambunan et al., 2019)

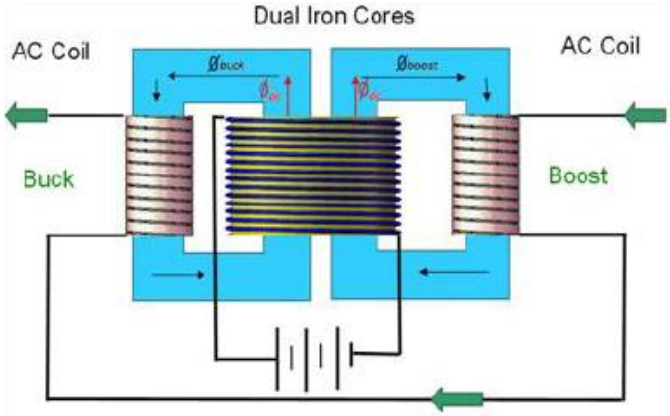

Fig. 2. 18: Iron core reactors (Tambunan et al., 2019)

The reactance of a CLR can be calculated using the formular below. This reactance value is calculated in order to determine the appropriate value to be used to achieve a desired fault current level (Razzaghi & Niayesh, 2011).

$$X_R = \frac{V_S}{\sqrt{3}}\left[\frac{1}{I_{SC_{Desired}}} - \frac{1}{I_{SC_{system}}}\right] \tag{2.6}$$

Where:

X_R – reactor reactance (Ω)

V_S – system voltage (V)

$I_{SC_{Desired}}$ – desired short circuit current

$I_{SC_{system}}$ – system short circuit current

2.6.7.2 Superconducting Fault Current Limiters (SFCL)

SFCL can be defined as a device which can be installed in an electric network to limit the undesirable current in the event a fault occurs. SFCL structures have good characteristics to control the fault-current levels due to their variable impedance in normal operation and fault condition. The design of SFCL has to be both flexible, to allow an easy adaptation to all applications of similar nature, and robust with high quality reproducible properties (Nemdili & Belkhiat, 2012).

There are two main types of SFCL, namely, the resistive Superconducting fault-current limiter (rSFCL) type and inductive Superconducting fault-current limiter (iSFCL) type. In the rSFCL type the superconductor is directly connected in series with the protected line/feeder and in the iSFCL type the superconductor is magnetically coupled into the protected line/feeder.(Nemdili & Belkhiat, 2012).

The method of operation for SFCL is based on superconductor material characteristic where they lose or gain their electrical resistivity under a certain temperature, current density, and magnetic field (Safaei et al., 2020a). During normal operation they will operate at very low impedance and when a fault occur, they switch to high impedance to limit the SCC (Safaei et al., 2020a).

The study shows that SFCL does not only limit the magnitude of SCC to a satisfactory level that can be handled by installed apparatus, but also damp transient recovery voltage. Furthermore, SFCL also improves the power system transient stability, power quality and reliability (Zhang, 2017).

a) Resistive Superconductive Fault Current Limiters (rSFCL)

The rSFCL are the most popular FCL and this is due to the discovery of High Temperature Superconductivity (HTS) in 1986 which drastically improved its ability to operate at high temperatures such as 70 Kelvins using less amount of superconducting material (Safaei et al., 2020a). The efficiency of their material significantly reduce their cost and that allows them to be commercially favourable (Safaei et al., 2020b).

Fig. 2. 19 shows the number of different FCL installed in the real power systems around the world and SFCL are leading the charts. Furthermore, Fig. 2. 20 zoom in to show that among the different types of SFCL the rSFCL are the ones that are mostly installed.

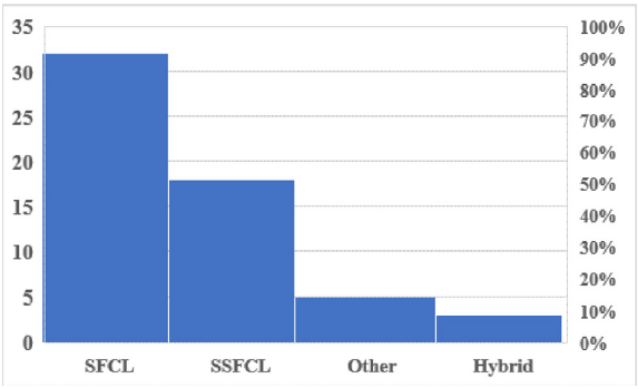

Fig. 2. 19: FCLs installed in power systems around the world till end of 2018 (Safaei et al., 2020b)

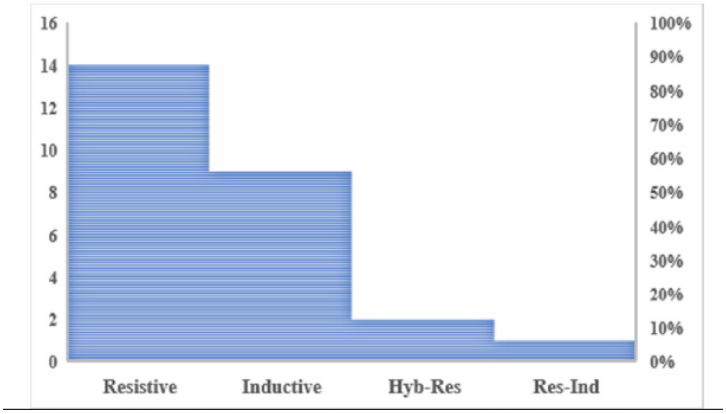

Fig. 2. 20: SFCLs installed in power systems around the world till end of 2018 (Safaei et al., 2020b)

- **Operation principle of rSFCL**

Fig. 2. 21 shows a single line diagram that demonstrate the operation principles of RSFCL. During normal operation of the grid, the superconducting material allows the current to flow through (Isc) without additional resistance into the system (Asghar, 2018). During a fault condition, the current increases drastically and causes the superconductor to quench thereby increases its resistance (Rsc) exponentially in proportion to the magnitude of the SCC (Eckroad, 2009).

The operating current of the rSCFL is determined by the operating temperature and the type of superconducting material used (Eckroad, 2009). The drastic increase of superconducting resistance subsequently increase the voltage across the superconductor and cause the current to flow towards the shunt which is a combination of resistor and inductor with in milliseconds where the SCC will be reduced (Eckroad, 2009).

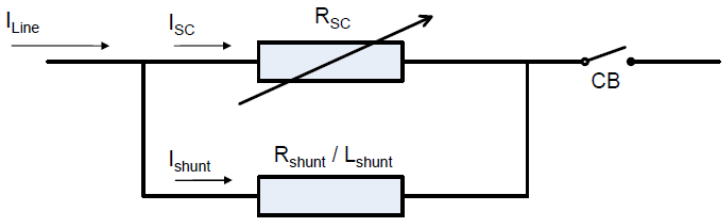

Fig. 2. 21: Resistive superconductive fault current limiters (RSFCL) (Eckroad, 2009)

When the HTS quench to transfer the SCC to the shunt, excessive heat occurs and create 'hot spot' issues and this is one of the challenges that was faces by the early designs of rSFCL (Eckroad, 2009). (Asghar, 2018) argues that rSFCL produce uneven heating during the quenching process. And that damages the HTS material, which then causes high power losses. The recovery time after a fault has occurred could also be several minutes of which that is inadequate for energy sources such as wind farms, to maintain grid voltage stability. However, (Noe, 2017) presented designs of rSFCL that entails advanced cooling systems of HTS material such as cooling systems with cold heads, storage dewer, small cyo-plant, and interface with a separate vessel as demonstrated in Fig. 2. 23 (Noe, 2017).

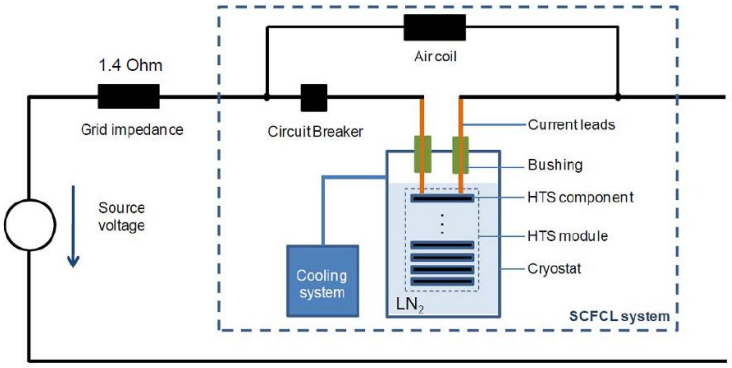

Fig. 2. 22: Resistive superconductive fault current limiters (RSFCL) Design of (Noe, 2017)

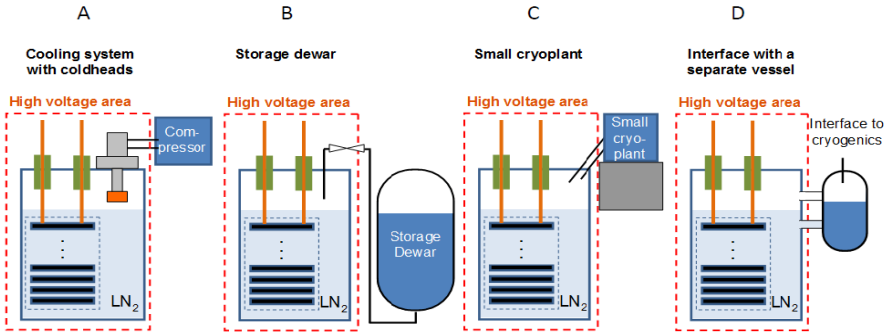

Fig. 2. 23: Cooling options for RSFCL (Noe, 2017)

According to (Noe, 2017) the formular below can be used to calculate the total power loss of a SFCL.

$$P = f\mu_0 {I_c}^2 [\frac{2}{\pi a^2} \int_c^a (a-x) tanh^{-1} \sqrt{\frac{sinh^2 \frac{\pi c}{D} - sinh^2 \frac{\pi c}{D}}{sinh^2 \frac{\pi a}{D} - sinh^2 \frac{\pi c}{D}}} dx + \frac{d}{12a} \left\{ 1 - \frac{c}{a} + \frac{8}{\pi^3 a} \int_0^c [\, tan^{-1} \sqrt{\frac{sinh^2 \frac{\pi a}{D} - sinh^2 \frac{\pi c}{D}}{sinh^2 \frac{\pi c}{D} - sinh^2 \frac{\pi x}{D}}} \right] dx \}] \quad (2.7)$$

According to (Asghar, 2018) the resistivity of the HTS material is a binary product of temperature and current density. And it can be calculated using the equation below.

$$P = pc(\frac{J}{Jc})^{n-1} \quad (J > Jc, T < Tc \quad (2.8)$$

$$P = 0 \quad (J < Jc, T < Tc \quad (2.9)$$

$$P = P_{HTS}(T) \quad T > Tc \quad (2.10)$$

Where:

ρc	=	$\frac{Ec}{Jc}$	=	Critical resistivity
Jc	=	$\frac{Jc0(Tc-T)}{(\mathrm{Tc-Top})}$		
$Jc0$	=	Critical current density		
n	=	Exponential index		
Top	=	Operational Temperature		

b) Inductive Superconductive Fault Current Limiters (iSFCL)

- **Components of iSFCL**

The iSFCL consist of two coaxial windings and an additional magnetic core. The primary winding is constructed with copper (Cu) and secondary winding consist of a HTS as demonstrated in Fig. 2. 24. Due to hot sports that occur during quenching the superconductor element is cooled in a liquid nitrogen bath to temperatures as low as 77 K (-196.15 °C).

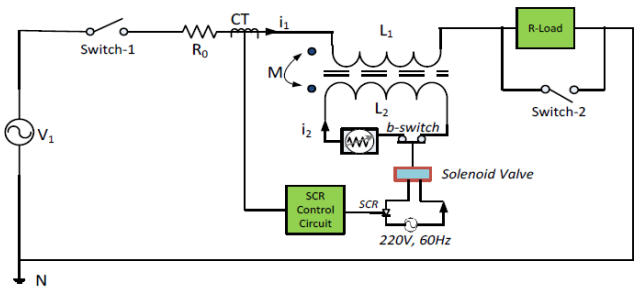

Fig. 2. 24: Transformer type iSFCL (Alam et al., 2018)

- **Configuration and Design of iSFCL**

The iSFCL can be built by making use of three different setups such as:

- Transformer-type iSFCL
- Rod-type iSFCL
- Magnetic shield iSFCL

The transformer type iSFCL, can further be configured into two different groups, namely superconductor connected in series with a transformer and two isolated windings.

- **Operation principle of iSFCL**

During normal operation of the network the iSFCL reflects the secondary impedance which is nearly zero. When a short circuit occur and the current of the network increases, the excitation of the primary winding occurs and the impedance of iSFCL increase drastically to limit the current (Alam et al., 2018).

The primary winding is connected in series with the load and the secondary winding is connected in series with the superconductor as demonstrated in Fig. 2. 24. When a short circuit occurs, superconductors in the secondary winding of the transformer will be quenched and limit the fault current. Subsequently the fault current will be limited in the primary winding as well (Alam et al., 2018).

In magnetic shield iSFCL configuration the cylinder acts as a shield for the field produced by an AC coil allowing current to flow through it and after a short circuit occurs, the superconductive cylinder dampens, and a magnetic path is created inside the cylinder which force current to flow through a high-impedance path and limiting the fault current. The rod-type iSFCLs can be considered to be a new version of the magnetic shield-based iSFCLs because in its design instead of using a ring-type core, a rode has been used (Safaei et al., 2020a).

- **Benefits of iSFCL**

Some of the advantage of a transformer type iSFCL is that it enhances the reliability of power system supply and provide power system stability.

c) Flux-locked type SFCL (FLSFCL)

- **Components of FLSFCL**

The FLSFCL type make use of magnetic coupling between windings that are placed on the same iron core and the two windings with different number of turns are in parallel with an HTS element is in series with secondary winding as demonstrated in Fig. 2. 25.

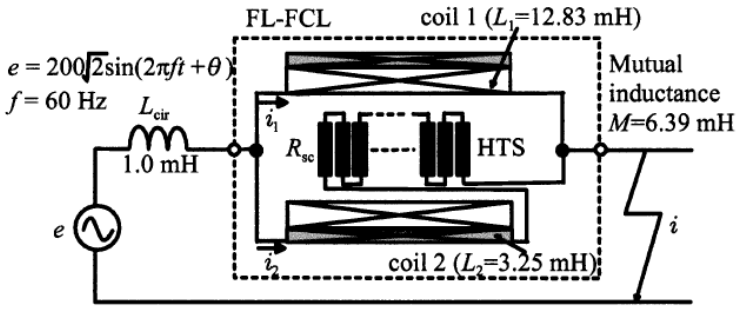

Fig. 2. 25: Configuration of a Flux-locked type SFCL (Matsumura et al., 2003)

- **Configuration and Design of FLSFCL**

There are different configurations to the design of FLSFCL available such as:

- The iron core with three wounded coils
- Series resistor
- Backup magnetic field coil for HTS element

- **Operation principle of FLSFCL**

When the linkage flux is maintained, the voltage across all three windings is measured to be zero. Therefore, the FLSFCL has less impedance in normal operation. Under fault condition an ac magnetic field coil is connected to the third winding and increases the impedance of HTS element to quench fault current.

Fig. 2. 25 demonstrate a configuration of FLSFCL with two coaxial coils (coil 1 and coil 2) and a HTS. The two coils are coupled in parallel to each other with HTS connected in series with coil 2. Under normal operation when a current that is below the value of a triggering current flows through HTS, the impedance of the HTS is very low. Because when two coils are coupled in parallel, the magnetic flux produced by each coil cancels out each other and that subsequently cause the voltage across both coils to be close to zero. Therefore, the lower the voltage, the lower the impedance.

When a fault condition occurs and the triggering current value has been exceeded, the resistance in the HTS will increase and that will result into imbalance of magnetic flux between the two coils. Consequently, a high impedance path will be created to limit the high fault currents (Matsumura et al., 2003). A much more recent and comprehensive review of the FLSFCL has been discussed on (Kim & Ko, 2021).

- **Benefits of FLSFCL**

Its ability to control initial limiting current level by adjusting the inductance between two coils is what makes them standout from other SFCL (Safaei et al., 2020a) and it has less power burden of the HTS (Alam et al., 2018).

d) DC reactor type SFCL (DCRSFCL)

- **Components of DCRSFCL**

The DCRSFCL make use of DC biased saturated core as the means to limit the fault current as demonstrated in Fig. 2. 26. The B-H curve of a magnetic circuit indicates that low inductance value is achieved in saturated region and very high value in unsaturated region of the core (Safaei et al., 2020a).

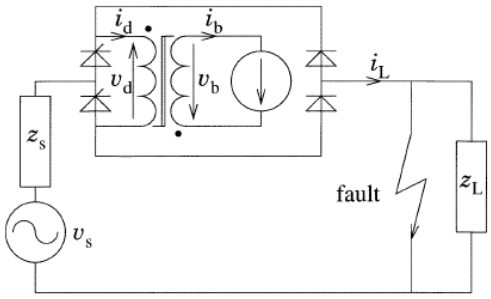

Fig. 2. 26: Saturated DC reactor type SFCL (Hoshino et al., 2003)

- **Configuration and Design of DCRSFCL**

The DCRSFCL can be designed using two kinds of DC-biased coils namely (Gonçalves Sotelo et al., 2022):

- Superconducting winding
- Conventional copper coil

- **Operation principle of DCRSFCL**

Under normal condition, the core is saturated with very low impedance, but when a fault occurs, the core becomes unsaturated due to high fault currents flowing in the circuit. When a core is unsaturated its inductance becomes very high and subsequently cause

high voltage drop in the line which causes the fault current to be limited (Safaei et al., 2020a).

During the limitation of the fault, when the iron core is driven from the saturated state to the unsaturated, that transition happens in a strong nonlinear manner, introducing harmonics in the line voltage. However, the main concern is not the harmonics rather the presence of voltages in the DC coil during the current limitation.

e) Vacuum Interrupter Based SFCL (VISFCL)

- **Components of VISFCL**

The VISFCL make use of superconductor, a vacuum interrupter, and bypass coil to limit fault currents. The vacuum interrupter is the main element in this type of SFCLs. The vacuum interrupter and superconductor are coupled in parallel with a bypass coil and that entirely act as a commutation switch as demonstrated in Fig. 2. 27 (Endo et al., 2008).

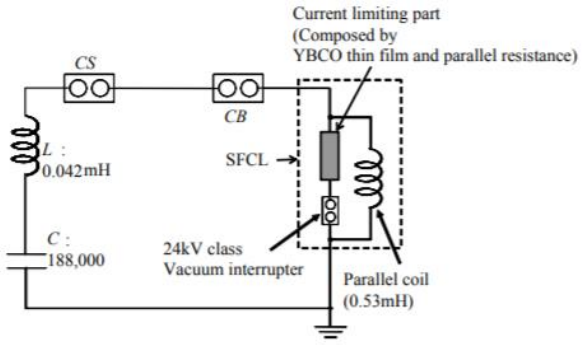

Fig. 2. 27: Circuit diagram of a Vacuum interrupter based SFCL (Endo et al., 2008)

- **Operation principle of VISFCL**

During normal operation of the circuit, the SFCL remains on superconducting state because the current flowing is below its critical current. The current will continue to flow through the vacuum interrupter and avoid the coil because that is a less resistive path.

In the event of fault, the superconductor will be quenched and activate the excretion mechanism of the vacuum interrupter, resulting to the vacuum interrupter to be opened. Subsequently the fault current will passe through the parallel coil where it will be limited (Safaei et al., 2020a).

It is important to note that when the SFCL switch to quenching mode, there are high temperatures that are generated by the spark in the vacuum interrupter and thermal management of a superconductor during the fault is one of the main problems with SFCLs. In VISFCLs, a vacuum tube-based strategy is used to reduce the high temperature (Safaei et al., 2020a).

f) Resonance type SFCL

- **Components of resonance type SFCL**

The resonance type SFCL make use of high impedance that is formed as a result of, resonance by inductor and a capacitor coupled in series or in parallel. This kind of SFCL is made up of a copper reactor, capacitor, superconductor, and ZnO arrester as demonstrated in Fig. 2. 28. The value of superconducting and a copper reactor is set to be nearly the same. The capacitor is designed to cancel the impedance of the superconducting reactor when the resonant frequency is in tune with the system frequency.

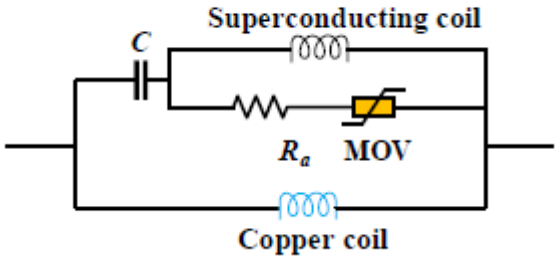

Fig. 2. 28: Resonance type SFCL (Guo et al., 2020)

- **Operation principle of resonance type SFCL**

During normal operation, the current flows through the capacitor and the superconducting reactor, with a very minimal amount flowing through the copper coil. Under this condition the arrestor will act as an open circuit with no current flowing through it. When a fault occurs, the voltage across the arrestor will increase above a critical value and short circuit, allowing a current to flow through. Under such condition, the resonant frequency will not be in tune with the system frequency. Therefore, the FCL will present a high impedance to the circuit, which will subsequently limit the fault current (Safaei et al., 2020a).

g) Matrix type SFCL (MSFCL)

- **Components of resonance type MSFCL**

Fig. 2. 29 illustrate an equivalent schematic diagram of a 3 x 3 Matrix type SFCL that is made up of “m” current limiting modules electrically linked in series with incoming node and outgoing node. The “n” number of current limiting matrix elements electrically linked in parallel. Each matrix element consist of a superconductor and an inductor linked in parallel (Mohseni et al., 2011).

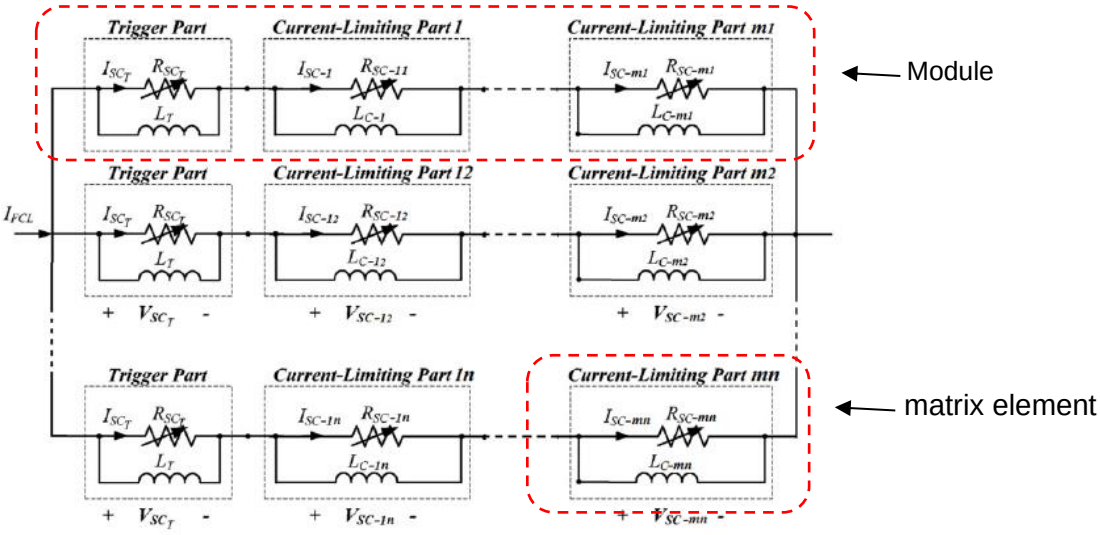

Fig. 2. 29: Equivalent circuit for a 3x3 Matrix type SFCL (Mohseni et al., 2011)

- **Operation principle of resonance type MSFCL**

During normal operation the current flows through a superconductor until a critical current value is reached. The superconductor is connected in parallel with a trigger coil and the trigger coil is magnetically connected to it. When a fault occurs, the superconductor will switch to resistive state and the SCC will generate a constant magnetic field in the trigger coil and lessen the voltage across the superconductor.

Thus, the superconductor will switch to quenching mode and limit the abnormal current (Safaei et al., 2020a). The number of rows in the matrix is calculated based on the amount of the nominal current and the number of columns current limiting impedance required for a particular network (Mohseni et al., 2011). Therefore, the bigger the circuit, the bigger the matrix.

2.6.7.3 Solid State Fault Current Limiters (SSFCL)

The SSFCL make use of semiconductor power switches (SPS) such as GTO, IGBT, and ICGT as the main elements to limit the fault currents (Gonçalves Sotelo et al., 2022) (Tambunan et al., 2019). The recent advancement in the SPS technology has developed new thyristors that operate at high voltage and current rating which subsequently put the SSFCL in a position to be commercially feasible (Tambunan et al., 2019) (Safaei et al., 2020b). SSFCL are less expensive, instant recovery after a fault, minimum losses, have flexible structure provided by modular structure of power electronics converters, and the advancement of semiconductor technology is growing at exponential rate when compared with other FCL technologies (Safaei et al., 2020b)(Patil & Thorat, 2017). However, the SSFCL have high switching losses which present harmonic problems in the circuit (Patil & Thorat, 2017).

a) Switched impedance SSFCL (SISSFCL)

The operational principle of SSFCL is that they are installed in the condition path of the flow of current in the circuit and are turned off instantaneously when the fault current occurs to dynamically insert additional impedance in the circuit that will limit the fault current (Safaei et al., 2020b) (Patil & Thorat, 2017).

Fig. 2. 30 demonstrate a typical SSFCL, at steady state of the system, the solid state switch is closed and provides a path to bypass the impedance and during a fault condition the solid state switch will be opened to force the fault current to flow through the impedance where it will be limited before it flows further to the grid (Gonçalves Sotelo et al., 2022).

An overcurrent detector scheme which is triggered by the SCC is usually used to open or close the switch depending on the critical current being exceeded or not. Auxiliary components like a snubber circuits and equalization resistors are negligible during normal operation of the circuit (Safaei et al., 2020a).

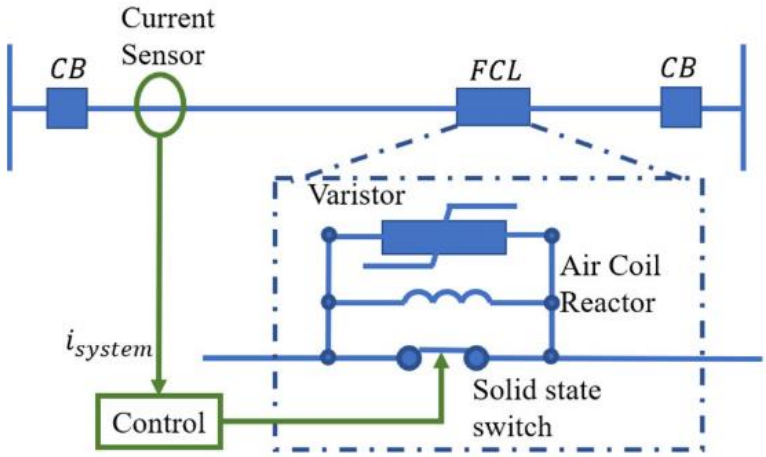

Fig. 2. 30: A series connection of SSFCL (Gonçalves Sotelo et al., 2022)

b) Bridge type SSFCLs (BSSFCLs)

- **Components of resonance type BSSFCLs**

The Bridge type SSFCLs make use of full-bridge solid-state switches with an inductor in the DC branch. Fig. 2. 31 is a circuit diagram that illustrate the Bridge type solid-state FCLs. where:

L_{dc}	-	Reactor
Z_f	-	Limiting impedance
Z_{no}	-	Varistor

Z_f provides a current path when a fault occurs and Z_{no} mitigates the over-voltage under the same condition. A common solid state switch was used in this diagram however, several other types of semiconductor switches can be utilised based on the proposed design. The use of different types of solid-state switches can help to cut costs and improve the overall performance of the FCL (Gonçalves Sotelo et al., 2022)

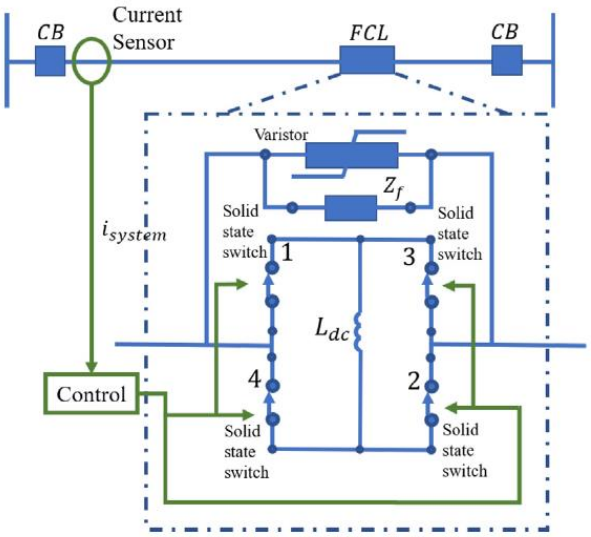

Fig. 2. 31: Bridge type solid-state FCLs (Gonçalves Sotelo et al., 2022)

- **Operation principle of resonance type BSSFCLs**

Under normal condition, all switches are operational, and the line current flows through switch #1, reactor Ldc, and switch #2 in the positive half wave and then flows through switch #3, Ldc, and switch #4 In the negative half-wave. There is constantly a DC current flowing through Ldc u under normal operation, due to positive and negative half wave alternation over it.

In an event of a fault, the Ldc avoids the fault current and, after the fault is detected by the current sensor, two switches are turned off (1 and 4 or 3 and 2) through the control circuit to force limited current in the Zf branch. The remaining switches remain on so the Ldc current can gradually discharge (Gonçalves Sotelo et al., 2022).

c) Resonance type SSFCLs (RSSFCLs)

- **Components of resonance type RSSFCLs**

The resonance type SFCL is based on the resonance effect for circuits that consist of inductors and capacitors (LC circuits). The LC circuits can be configured in series or parallel as demonstrated in Fig. 2. 32 (Gonçalves Sotelo et al., 2022).

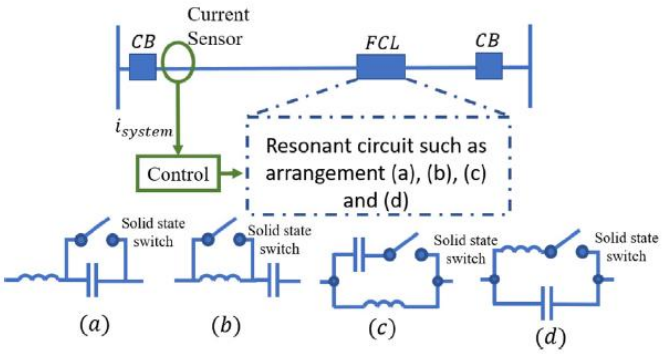

Fig. 2. 32: Schematic diagram of a Resonance type SFCL (Gonçalves Sotelo et al., 2022)

- **Operation principle of resonance type RSSFCLs**

The resonant frequency is one of the most important aspects of the resonance type SFCL as it is used in these circuit as a triggering factor to determine the equivalent impedance required in the circuit.

The resonant frequency is given by:

$$f_{RES} = \frac{1}{2\pi\sqrt{LC}} \tag{2.11}$$

During normal condition, the resonant frequency and the system frequency are in tune, meaning, the inductor and capacitor are at resonance with power delivering frequency. Henceforth, their reactance will cancel each other leaving only the normal impedance of the network in consideration.

When a short circuit occurs, the voltage of the series resonance fault current limiter will increase significant resulting into a current flowing through the switch. When current flows through the switch, a very small amount of current will flow through the capacitor. The low current flow through the capacitance will results to a disruption of series resonance if the inductor and capacitor, meaning the resonant frequency will not be in tune with the system frequency. Subsequently leading to increase in system impedance through the inductor and limiting fault current that is passing through (Eyuboglu et al., 2020).

d) Multicell type SSFCLs (MCSSFCLs)

- **Components of resonance type MCSSFCLs**

The MCSSFCL is made up of two fundamental parts, namely a transient cell (TC) part and a resistive cells (RC) part as illustrated in Fig. 2. 33. The two parts are linked in series connection to maintain high voltage operation standards. The TC part consist of two diodes (D1 & D2) and two transient limiting reactors (TLRs). The two TLRs are used to limit the transient fault current in an event a fault occurs. The RC part is made up of two

Gate Turn Off (GTO) semiconductor switches and a single current limiting resistor (Shafiee et al., 2020).

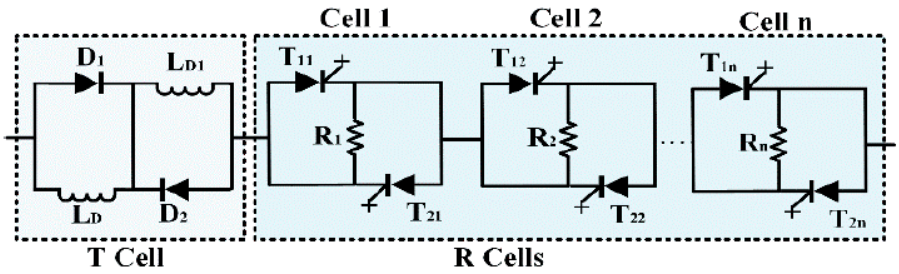

Fig. 2. 33: Multicell type SSFCL (Shafiee et al., 2020)

- **Operation principle of resonance type MCSSFCLs**

During normal operation, all RCs GTO switches closes, bypassing all RCs resistances (R1 - Rn). Therefore, the line current will flow through, D1 - LD1 - T11 - Tn and charge the inductor LD1 to its maximum charging current IL. The negative cycle will flow on the alternative path and charge the inductor LD2. When LD1 and LD2 are fully charged they act as a current source resulting to D1 and D2 to operate on freewheel due to very minimal voltage drop under normal operation (Shafiee et al., 2020).

When a fault occurs, the control system of the Multicell type SSFCL will switch off some of the GTO switched and introduce the RC resistors in the path of a fault current. Furthermore, the fault current will have to flow through LD1 or LD2, where it will be suppressed (Shafiee et al., 2020).

The number of series connected cells can be increased to achieve the application of MCSSFCL in very high voltage systems. The appropriate coordination and control of the cells still remain a challenge for the MCSSFCL (Safaei et al., 2020a).

2.6.7.4 Hybrid FCL

a) Bridge type HFCL

- **Components of Bridge type HFCL**

The hybrid FCLs are a combination of SFCLs and SSFCL. Its basic design is based on using a superconductor current limiting coil and usually a thyristor-based bridge as demonstrated in Fig. 2. 34. Thus, these FCLs enjoy the advantages of both SFLs and SSFCLs (Safaei et al., 2020a). A bias voltage source was introduced to isolate the inductor from being connected directly to the load, because under such condition, the inductor would limit the current flow to the load.

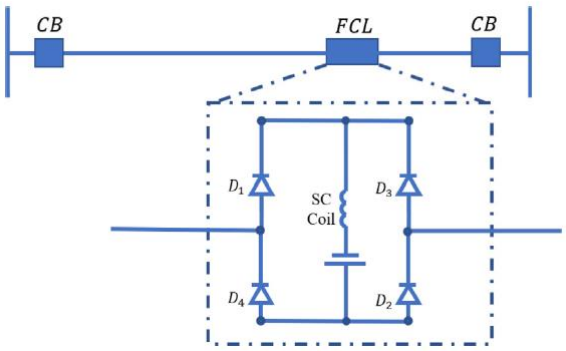

Fig. 2. 34: Diode Bridge and Superconducting Coil Bridge type hybrid FCL (Gonçalves Sotelo et al., 2022)

- **Operation principle of Bridge type HFCL**

Under normal operation, the voltage source produces a bias DC current in the inductance (IL) to polarize the diodes. IL is set to a value (Io) which must be greater than the maximum peak value (Imax) of alternate current during steady state. The voltage of the bias source is only enough to supplement the voltage drop across the diodes. Therefore, only the DC Io current can flow through the inductance with a minimal voltage drop during steady state.

In the event of a fault, Imax exceed I0 and a pair of diodes strings (D1 and D2 or D3 and D4) ceases to conduct in part of the current cycle, and the inductance is introduced to limit the current towards the load (Gonçalves Sotelo et al., 2022).

b) Non-inductive HFCL

- **Components of Non-inductive HFCL**

Fig. 2. 35 demonstrate an equivalent diagram of a non-inductive type SFCL, which consist of a pair of superconducting coils, namely a fault current limiting coil as well as a trigger coil. The two coils are linked in anti-parallel and are magnetically coupled with similar self-inductance. Which means that they share a similar potion of line current.

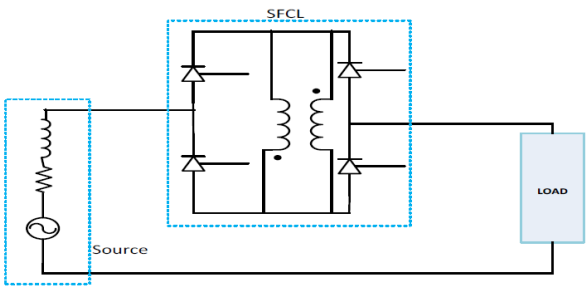

Fig. 2. 35: Non-inductive type FCL (Alam et al., 2018)

- **Configuration and Design Non-inductive HFCL**

Different types of configurations can be used on this type of FCL such as:

- Coaxial coil configuration
- Bifilar winding configuration

When coaxial coil configuration and a bifilar winding configuration are compared to each other, a bifilar winding configuration is a preferred option to achieve high impedance ratio (Alam et al., 2018).

- **Operation principle of Non-inductive HFCL**

When a fault occurs, the current flowing through the trigger coil reaches a critical current value, causing it to switch from superconducting state to normal model. This changes the current ratio of the coils, which makes the flux of the reactor to rise. Consequently, the equivalent impedance of the coils rises, resulting to limitation of the fault current (Safaei et al., 2020a).

2.6.7.5 Other technologies

The following are other fault current limiting technologies which have been discussed into details on (Tambunan et al., 2019), (Gonçalves Sotelo et al., 2022), (Guillen et al., 2020), (Alam et al., 2018), (Safaei et al., 2020b), and (Patil & Thorat, 2017). Some of these technologies are still under development and some are commercially available. The selection of use depends on the type of circuit where the FCL will be applied.

a) Pyrotechnic Current Limiters (PCL)
b) Permanent magnet-based DC FCL
c) Pre-saturated/saturated single phase FCL
d) Five-leg saturated core based FCL
e) Low-permeability type FCL
f) Electrodynamic type FCL
g) PTC-resistor based FCL
h) Capacitor-based SSFCL (CBSSFCL)
i) Magnetic turn-off SSFCL (MTSSFCL)
j) Impedance-based SSFCL (SBSSFCL)
k) Liquid metal FCL

2.6.8 Fault current limiters control strategies

(Wang et al., 2023) propose a new FCL based on self-driving rheostat. This literature argues that; (1) The wildly used current limiting reactors can inhibit the switching inrush current, undesirable SCC, and has good economic feasibility. However, its long-time series connection to the network produce significant losses (Wang et al., 2023); (2) The proposed

zero-loss type which only connects the reactor to the grid during fault condition does eliminate the operational losses. However, it cannot limit the first half-wave peak of fault currents due to the delay time of mechanical switches (Wang et al., 2023); (3) Superconducting fault current limiters (SFCL) has a disadvantage of large heat generation and the proposed temperature control systems bring a huge economic Budden (Wang et al., 2023); (4) The Solid-state fault current limiters (SSFCL) has immense state losses (Wang et al., 2023). Therefore, (Wang et al., 2023) propose a self-driving FCL that has zero losses, utilizes the energy of the short circuit to operate, and can counter all shortfalls of the above-mentioned devices. Fig. 2. 36 shows the structure of the proposed SD-FCL.

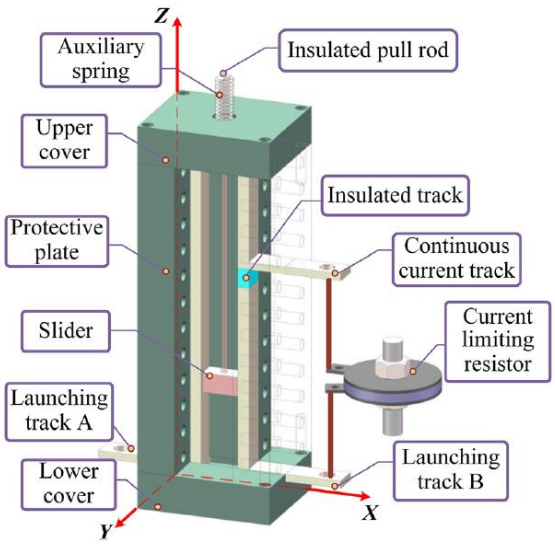

Fig. 2. 36: Structure of the Proposed SD-FCL (Wang et al., 2023)

(Fang et al., 2023) propose Fault Current Limitation Control (FCLC) to be used to improve the utilization of fault ride-through of multiple RES. Fig. 2. 37 shows a typical microgrid that has a grid supply, Point of Common Connection (PCC), Grid Side Converter (GSC), Distributed Generation units (DG), and a flow of fault current.

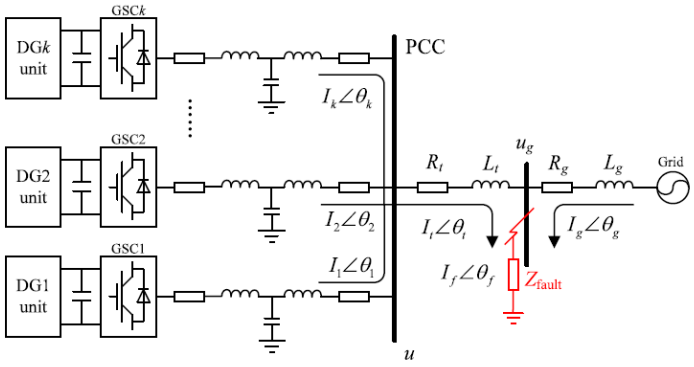

Fig. 2. 37: Micro-grid with Distributed Generation (Fang et al., 2023)

Fig. 2. 38 shows a similar microgrid as Fig. 2. 37 but with FCLC connected to the grid.

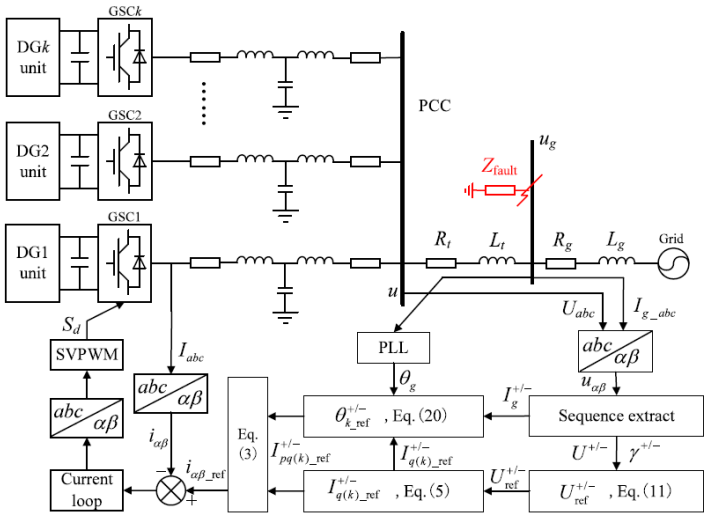

Fig. 2. 38: Microgrid with a connected FCLC (Fang et al., 2023)

Fig. 2. 39 shows a phasor diagram of the fault current angle and amplitude that is injected into the fault as shown in Fig. 2. 37 and Fig. 2. 38. “If” is the fault current measured without FCLC and “If-new” is the fault current measurement with FCLC. In this phasor diagram, it can be observed that the FCLC enables significant fault current reduction in the network.

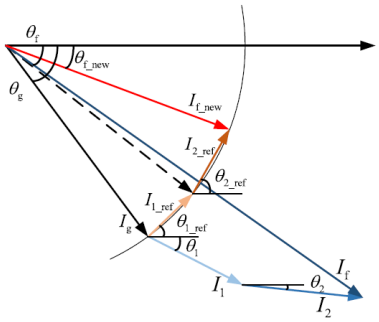

Fig. 2. 39: Phasor diagram of fault current amplitude with and without FCLC (Fang et al., 2023)

The literature in (Liu et al., 2019) agrees with the literature in (Fang et al., 2023) however, (Liu et al., 2019) further propose technics like fault current secondary limitation control (FCSLC), fault current tertiary limitation control (FCTLC), and fault current quartus limitation control (FCQLC).

2.6.9 Comparison of FCLs

FCL are divided into two main groups, namely superconducting FCL and non-superconducting FCL. These two groups differ from one another as far as the size, cost, power losses, short circuit monitoring and control systems, and topology complexity is concerned. Table 4 gives a comprehensive comparison between the two groups.

Table 4: Comparison between superconducting FCL and non-superconducting FCL (Alam et al., 2018)

Items	Superconducting FCL	Non-Superconducting FCL
Size(m^2) and weight(kg)	Big & substantial weight	Little and light weight
Cost ($)	High implantation cost caused by expensive superconducting apparatus (Inductor and Resistor)	Low in cost since they do not have superconducting material. Only required resistor and inductor.
Power Losses	No losses during normal operation, except for inductive type SFCL	There are losses during normal operation of the electric network
Practical installation status	Some such as Hybrid, saturated iron core, and rSFCL already been installed by grid owners	Still under development
Interruption with nearby communication lines	It does interrupt the nearby communication lines	It does not interrupt the nearby communication lines
Short circuit monitoring and control systems	No additional short circuit detection and control system needed	Additional short circuit detection and control system is needed
Topology complexity	Many of them has sophisticated circuit topology	Very simple topology for most of them

Table 5 further zoom into different types of superconducting FCL such as resistive, inductive, transformer, magnetic shield, flux lock, non-inductive, hybrid SFCL and compare them based on advantages and disadvantages.

Table 5: Comparison of different SFCL by advantages and disadvantages (Alam et al., 2018)

SFCL Types	Advantages	Disadvantages
Resistive	❖ Can recover automatically ❖ Faster SCC limiting capabilities ❖ Little in size ❖ Cost less ❖ Less complex structure/design	❖ Requires stretched length of superconductor for high voltage implementation ❖ Dissipates large power and take long to recover ❖ Simultaneous quenching cannot be performed due to critical current mismatch between installed units
Inductive	❖ Less weight and device size are small due to coreless design.	❖ Power losses during stand-by mode caused by leakage reactance ❖ Conventional circuit breaker is required to switch off SC

		to avoid maximum HTS winding temperature.
Transformer	❖ Applicable in wide range of current limiting ❖ Less recovery time	❖ Takes long to initiate FCL ❖ High power burden of SFCL
Magnetic Shield	❖ Uses magnetic shielding body to detect SCC, no additional fault detection devices required ❖ Flexibility design due to turn ratio It provides isolation layer between SFCL and electric network	❖ High voltage drops under normal operation ❖ Dissipates magnetic field interrupts the operations of nearby sensitive devices
Flux-lock	❖ Operating current can be changed ❖ Low power load on superconducting items	❖ Huge size ❖ Significant weight ❖ Expensive
Non-inductive	❖ Costs less ❖ Recovers fast ❖ Minimal AC losses ❖ Operates in very high voltages	❖ High amount of cryogenic ❖ High circulating current and leakage inductance
Hybrid	❖ Synced quenching can be performed ❖ Requires minimal length of superconductor for high voltage and current applications	❖ Replacement of liquid nitrogen is required if the line has been off for a long time

2.7 Summary

In this chapter, the literature of short circuit, major SCC contributors, different techniques to reduce SCC, and classification of FCLs was discussed. The Phase – Phase, Phase – Phase – Ground, Three Phase – Ground, Phase – Phase – Phase, and Sensitive Earth fault are the common faults that occurs in the power system. Distributed generation and bulk integration of RES are the major causes of increased levels of SCC. Network reconfiguration or adding additional impedance to the network is some of the available techniques to reduce SCC. The use of FCLs is a better option to increase the grid's impedance because they operate at a very low impedance during normal operation and switch to very high impedance when a fault occurs. FCLs can be classified either as passive or active based on the topology used.

Furthermore, a broad literature of FCL was covered in this chapter with an attempt to find the best FCL that can solve the problem of increased SCC levels. Topics such as, attributes of a good FCL, advantages of FCL, disadvantages of FCL, attributes to be considered when choosing a FCL, application of FCL, case studies where FCL have been utilised, classification of FCL, different types of FCL, FCL control strategies, and comparison of FCL were covered. This review has given an arial view of where the FCL technologies stand to date and rSFCL are currently the type of technology that has advanced very well following its ability to quench at very high temperatures.

CHAPTER 3: Mathematical Modelling and simulation

3.1 Introduction

A mathematical model is used when solving complex engineering problems to examine, analyse and predict behaviour and events. In this chapter the mathematical expression of Periodic and Aperiodic components of SCC, SCC on simplified power system, E – J Characteristic, and determination of shunt resistance will be discussed. Furthermore, Modelling and Simulation of rSFCL will be discussed. MATLAB Simulink is used as a simulation software to simulate different scenarios of the rSFCL model.

3.2 Periodic and Aperiodic components of SCC

According to (Zhang, 2017) a continuous injection of current has to be maintained before and after a short circuit has occurred in the power system. However, the periodic components of the current before and after short circuit is not identical due to a self-inductance current that occur after a short circuit. Lenz's law explains that an aperiodic component of short circuit current is observed after a short circuit has occurred and it is caused by the self-inductance current.

The following single line diagrams, equations, and phasor diagrams illustrate the mathematical expression of the current before and after a fault occurs.

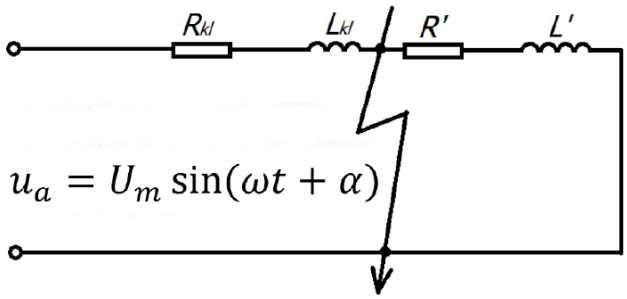

Fig. 3. 1: Single line diagram of power system with a fault (Zhang, 2017).

Fig. 3. 1 shows a single line diagram that can be used to analyse the transient state of a single-phase SCC.

During normal operation, the source voltage is expressed as:

$$u_a = U_m \sin(\omega t + \alpha) \quad (3.1)$$

The line current is defined as shown in equation (3.2), where I_m is the amplitude of the line current.

$$i = I_m \sin(\omega t + \alpha - \varphi) \quad (3.2)$$

I_m is defined as:

$$I_m = \frac{U_m}{\sqrt{(R_{kl} + R')^2 + \omega^2 (L_{kl} + L')^2}} \tag{3.3}$$

φ is the angle of the source impedance and it is defined as:

$$\varphi = tan^{-1} \frac{\omega(L_{kl} + L')}{R_{kl} + R'} \tag{3.4}$$

φ can also be defined as the angle by which the current lags the voltage.

Fig. 3. 2 below illustrates the relationship between the voltage angle and the impedance angle.

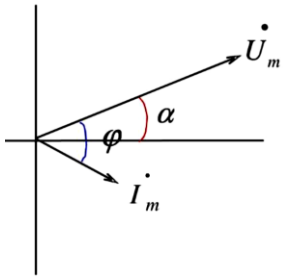

Fig. 3. 2: Phasor diagram of α and φ (Zhang, 2017)

When a short circuit occurs as demonstrated on Fig. 3. 1, the load impedance will be ignored and that will cause a sharp increase on the line current. However, the infinite source voltage will remain the same and expressed as:

$$u = U_m \sin(\omega t + \alpha) = R_{kl} i_k + L_{kl} \frac{d_{i_k}}{dt} \tag{3.5}$$

Therefore, the transient current is defined as:

$$i_k = \frac{U_m}{Z_{kl}} \sin(\omega t + \alpha - \varphi_{kl}) + ce^{-\frac{t}{T_k}} = I_{pm} sin(\omega t + \alpha - \varphi_{kl}) + ce^{-\frac{t}{T_k}} \tag{3.6}$$

Where I_{pm} is:

$$I_{pm} = \frac{U_m}{Z_{kl}} = \frac{U_m}{\sqrt{{Z_{kl}}^2 + (\omega K_{kl})^2}} \tag{3.7}$$

The impedance angle after the short circuit has occurred is defined as:

$$\varphi_{kl} = arctan\frac{\omega L_{kl}}{R_{kl}} \quad (3.8)$$

T_k as shown in equation (3.6) is a time constant after the short circuit has occurred and it is defined as:

$$T_k = \frac{L_{kl}}{R_{kl}} \quad (3.9)$$

To demonstrate the Lenz's law concept that the continuous injection of current is maintained before and after the SC occurs *t=0* is substituted on equation (3.2) and (3.6) and the new equations are:

$$i_{0+} = I_m sin(\alpha - \varphi) \quad (3.10)$$

$$i_{0-} = I_{pm} sin(\alpha - \varphi_{k1}) + c \quad (3.11)$$

Where, i_{0+} is the momentary current before SC occurs, and i_{0-} is the momentary current after the short circuit occurred.

The constant *c* is defined as:

$$c = I_m sin(\alpha - \varphi) - I_{pm} sin(\alpha - \varphi_{k1}) = i_{ap0} \quad (3.12)$$

Therefore, the value of SCC can be obtained by substituting equation (3.12) to equation (3.6) as shown below.

$$i_k = I_{pm} sin(\omega t + \alpha - \varphi_{kl}) + ce^{-\frac{t}{T_k}} \quad (3.13)$$

$$= I_{pm} sin(\omega t + \alpha - \varphi_{kl}) + [I_m sin(\alpha - \varphi) - I_{pm} sin(\alpha - \varphi_{k1})]e^{-\frac{t}{T_k}}$$

$$= i_p + i_{ap}$$

Where, i_p is a periodic component defined as follows:

$$i_p = I_{pm} sin(\omega t + \alpha - \varphi_{kl}) \quad (3.14)$$

And i_{ap} is the aperiodic component defined as follows:

$$i_{ap} = [I_m sin(\alpha - \varphi) - I_{pm} sin(\alpha - \varphi_{k1})]e^{-\frac{t}{T_k}} \quad (3.15)$$

Fig. 3. 3 demonstrate the periodic and aperiodic components of SCC as expressed on the equations above.

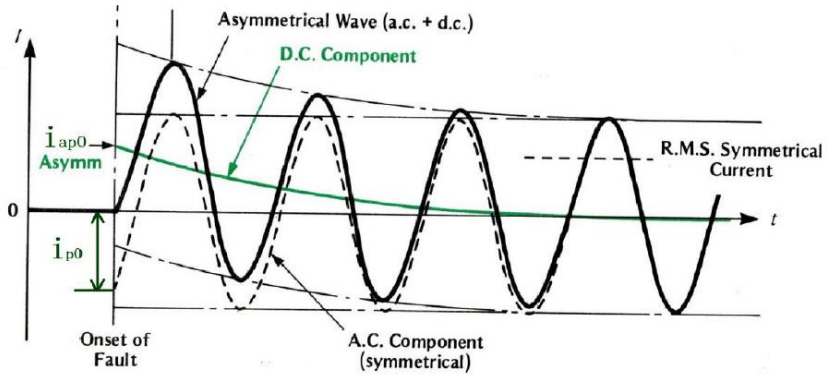

Fig. 3. 3: Illustration of periodic and aperiodic components of SCC i_p and i_{ap} (Zhang, 2017)

3.3 SCC of simplified power system

Fig. 3. 4 and Fig. 3. 5 show a simplified power system with and without a FCL installed. where V_s is a rated source voltage, Z_s is an internal impedance, Z_{load} is the load impedance, and Z_{fault} is the fault impedance. The magnitude of the line current I_{line} can be calculated by using equation (3.16), (3.17), and (3.18) below.

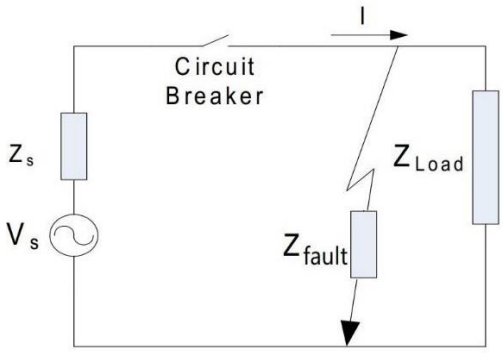

Fig. 3. 4: Simplified power network without FCL (Zhang, 2017)

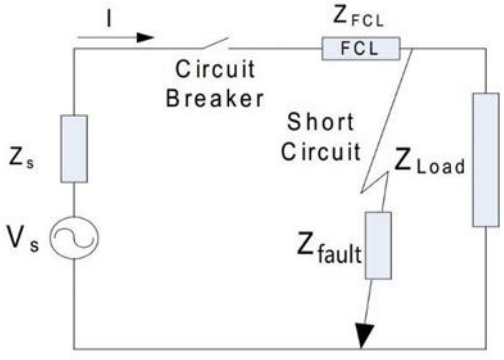

Fig. 3. 5: Simplified power network with FCL (Zhang, 2017)

When the power system is at steady state and there is no fault condition present, the line current is defined as:

$$I_{line} = \frac{V_s}{Z_s + Z_{load}} \tag{3.16}$$

When the power system is at steady state and a fault condition is suddenly introduced as shown in Fig. 3. 4, the line current will be defined by equation (3.17) where the load impedance is greater than the fault impedance. With such substantial decrease of impedance in the circuit, the line current will subsequently increase significantly.

$$I_{line} = \frac{V_s}{Z_s + Z_{fault}} \ , where \ Z_{fault} < Z_{load} \tag{3.17}$$

A FCL is installed as shown in Fig. 3. 5 where a SFCL impedance is introduced to limit the sudden high fault current. Therefore, the line current will be defined by equation (3.18).

$$I_{line} = \frac{V_s}{Z_s + Z_{SFCL} + Z_{fault}} \tag{3.18}$$

3.4 E-J Characteristic

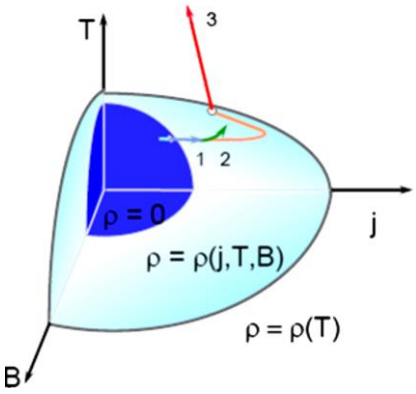

Fig. 3. 6: The characteristics of HTS material (Nemdili & Belkhiat, 2012)

Fig. 3. 6 illustrate the Temperature, Magnetic Field, and Current Density (T–B–J) characteristics of the High Temperature Superconductor (HTS) material. For the HTS to enable the resistive mode, the current density of superconductor would have to exceed the critical current density (Jc) in an event a fault occurs. Three operating states are demonstrated by “1”, “2”, and “3” where, “1” is a low resistance state, “2” is a normal operation state and “3” is a high inductance state. It is observed that the increase in the current density (J) is directly proportional with the increase in temperature, as well as the magnetic flux density. When the current density exceeds the pre-defined critical current density, the superconductor immediately switch to a high inductance state, and subsequently limit the SCC to a lower value. (Nemdili & Belkhiat, 2012).

Fig. 3. 7 is an E(j) Characteristics which demonstrates the behaviour of rSFCL. This characteristic is subdivided into three regions and each region can be express by power laws as shown in equation (3.19), (3.20), and (3.21).

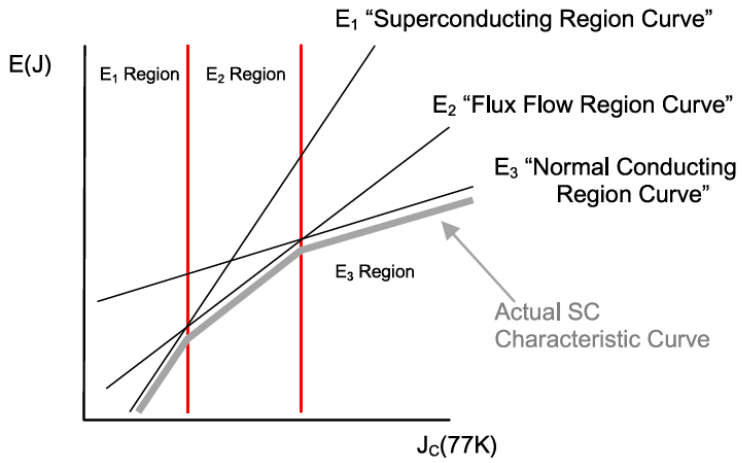

Fig. 3. 7: E(j) Characteristics (Nemdili & Belkhiat, 2012)

3.4.1 Superconducting region

$$E_1 = E_c \left(\frac{J}{J_c(T)}\right)^{\alpha(T)} \tag{3.19}$$

3.4.2 Flux Flow Region

$$E_2 = E_0 \left(\frac{E_c}{E_0}\right)^{\beta/\alpha(77\,K)} \left(\frac{J_c(77\,K)}{J_c(T)}\right) \left(\frac{J}{J_c(T)}\right)^{\beta} \tag{3.20}$$

3.4.3 Normal Conducting Region

$$E_3 = p(T_c)J \tag{3.21}$$

In these three equations, the electrical field and temperature have a major contribution in the performance determination of the superconductor as the variable impedance of the superconductor is largely influenced by them. The current density also plays a major role in characterising the nonlinearity of the superconductor.

During normal operation, when the rSFCL is installed in the power system, the three equations are continuously calculated to determine the region in which the SFCL is operating at. All the values obtained from the calculations are used as inputs of a comparator.

$J_c(T)$ critical current density is defined as:

$$J_c\,(T) = \left[\frac{(T_c - T_{sk})}{(T_c - V_n)}\right] J_c\ 77\ K \tag{3.22}$$

Where, T_c is a critical temperature and T_{sk} is there actual temperature.

R_s is the variable resistance used to simulate the SFCL and it is defined as:

$$R_s\,Thermal = \frac{D_{22}}{4K_s D_{21}\,L} \tag{3.23}$$

Where, D_{21} and D_{22} are the length and width of the superconducting tape.

L is the length of the superconducting coil.

3.5 Determining optimum shunt resistance

The optimum shunt resistance for a rSFCL can be determined through three standard operating zones, namely the superconducting zone, flux zone, and normal zone (Hooshyar et al., 2009).

The optimum shunt resistance is required due to the following factors (Hooshyar et al., 2009):

- The SCC levels are very high in transmission network. Therefore, the HTS temperature is also high. Thus, the cooling period of the rSFCL is very long. Subsequently, the time taken for the rSFCL to return to superconducting also increase. By making use of the shunt resistance as a limiting device, a parallel path for fault current to flow through is created. The HTS temperature will be reduced, and it will cool down more quickly after the short circuit has been eliminated (Hooshyar et al., 2009).

- The increased SCC levels and the subsequent temperature increase exposes the chemical structure of the HTS to high risk of deterioration. A deterioration that is severe enough may prevent the rSFCL from returning to superconducting zone (Hooshyar et al., 2009).

- The optimum value of shunt resistance is directly proportional to the growth of the power system. As more energy sources are integrated into the network and transmission and distribution network is expanded, the optimum shunt resistance must adjust in proportion to that change. Necessary calculations of the shunt resistor have to be done every time a significant change is done in the network so the system apparatus can remain protected and protection settings remain the same (Hooshyar et al., 2009).

Fig. 3. 8 is a typical graph that demonstrate the behavior of the rSCFL when a short circuit occur.

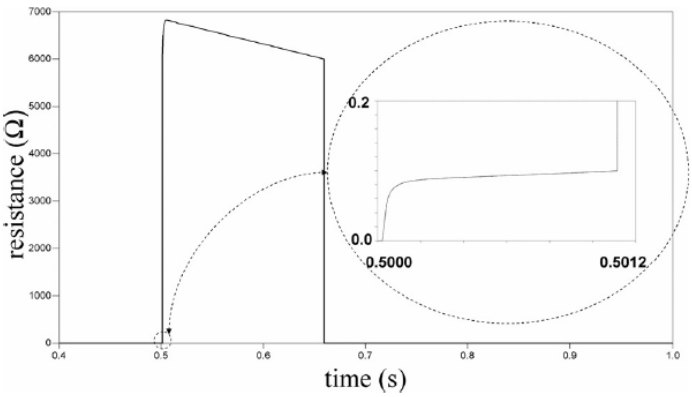

Fig. 3. 8: Behaviour of rSFCL under fault condition (Hooshyar et al., 2009)

3.5.1 Superconducting zone

The superconducting zone is when the measured current and temperature of the High HTS are both under their critical points as predefined (Hooshyar et al., 2009). The optimum resistance under this zone is defined as follows:

$$R_{rSFCL} = 0 \quad if\ i_{sc} < I_c\ and\ T < T_c \tag{3.24}$$

Where:

R_{rSFCL} = Shunt resistance
i_{sc} = Short circuit current
I_c = Critical current
T_c = Critical temperature
T = Measured HTC temperature

3.5.2 Flux zone

The flux flow zone is when the measured current exceeds the predefined critical current I (I_c) and the temperature of the HTS is less than the predefined critical temperature (T_c) (Hooshyar et al., 2009). The optimum resistance under this zone is defined as follows:

$$R_{rSFCL} = \{\frac{J_{c0}}{|j|}\left(\frac{T - T_b}{T_c - T_b} - 1\right) + 1\}\frac{pf{J^2}_{c0}V_{sc}}{{I^2}_c} \tag{3.25}$$

$$if\ i_{sc} < I_c\ and\ T < T_c$$

3.5.3 Normal zone

The normal zone is when the measured current exceeds the predefined critical current (I_c) and the temperature of the HTS also exceeds the measured predefined critical temperature (T_c) (Hooshyar et al., 2009). The optimum resistance under this zone is defined as follows:

$$R_{rSFCL} = pn\left(\frac{T}{T_c}\right)\frac{V_{sc}}{A^2{}_{sc}} \qquad is\ T > T_c \tag{3.26}$$

3.6 rSFCL Model

The Modelling and Simulation of an engineering concept is one of the highly valued stages when conducting and engineering research. It provides additional insights that are often impractical or impossible to discover/demonstrate through real-world experimental and theoretical analysis alone.

The model was done based on specific desired outcome which is to have a FCL that have nearly zero impedance during normal operation of the network, and adequately high impedance during a faulty condition.

3.6.1 Model specifications

Fig. 3. 9 is a MATLAB Simulink schematic diagram that was designed to simulate a rSFCL for this study. In this model a Controlled Voltage Source (CVS) that is equivalent to a controlled variable resistance was used as the main component to limit the SCC. The output of the controlled voltage source is driven by different variables, namely, input current, triggered critical current, and temperature value.

This model starts off by measuring the nominal current with a current measurement and calculate its RMS value. The RMS value is then used as in input to a MATLAB function block where the critical current and critical temperature is monitored. The specifications of the function block are shown in Fig. 3.10.

The resister “R” which is the output of the function block as shown in Fig. 3. 9, is a function of Current “I” and temperature “T”. If the measured RMS current is less than 200 A and the input temperature is also less than 77K, the value of “R” is set to be 0.01Ω. In this case, the resistor value is very small because it represents the superconducting state of the rSFCL where there is no fault in the network.

If the measured RMS current is greater than 200 A and the input temperature is greater than 77K, the value of “R” is set to be 50Ω. This is regarded as a condition where a fault has occurred and the rSFCL is on quenching state, adding more impedance in the network

to limit the fault current. Both “I” and “T” have to be greater than the critical setting for a quenching state to be initiated. When there is no “I” and “T” input, the value of “R” is set to be 0 Ω.

The adequate value of “R” is then multiplied with the SCC as stated by ohms law to get a voltage value that controls the CVS. R1 and R2 are both initial resistance of the rSFCL and are set to 0.005Ω each. The model is set to take approximately 2 ms to transition from superconducting state to quenching state. And it will take approximately 10 ms to recover back to normal operation after the fault has been cleared.

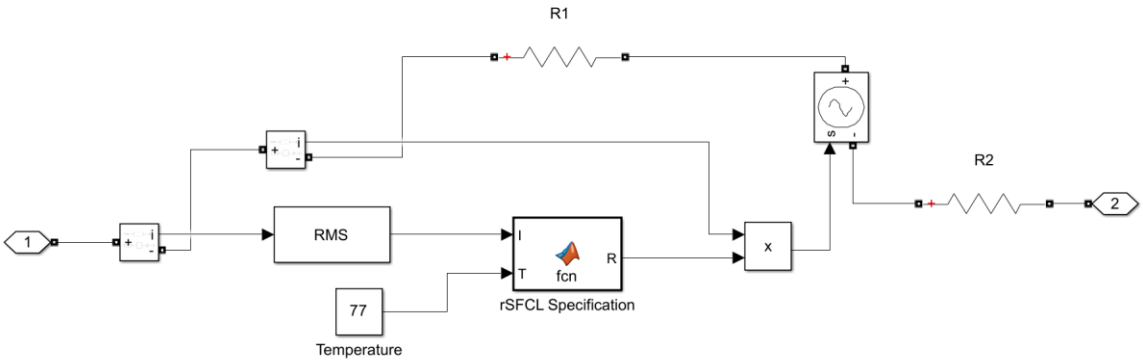

Fig. 3. 9: MATLAB Simulink schematic diagram of a rSFCL

Fig. 3. 10 shows the function block algorithm that process the input current and temperature, and issue out adequate impedance. The temperature is obtained from a constant input block which in real life is represented by a thermometer placed in a rSFCL.

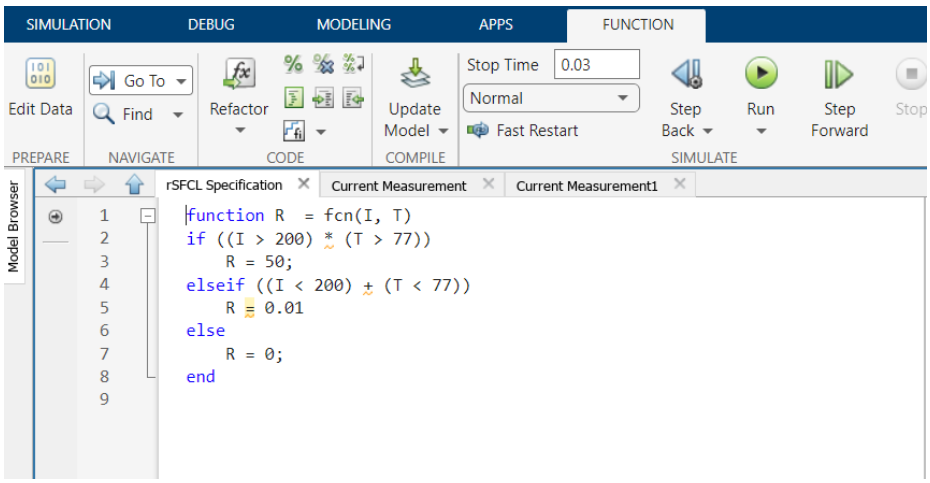

Fig. 3. 10: Function block algorithm

Fig. 3. 11 is a flow chart diagram that demonstrate the chain of commands that the rSFCL operated based on.

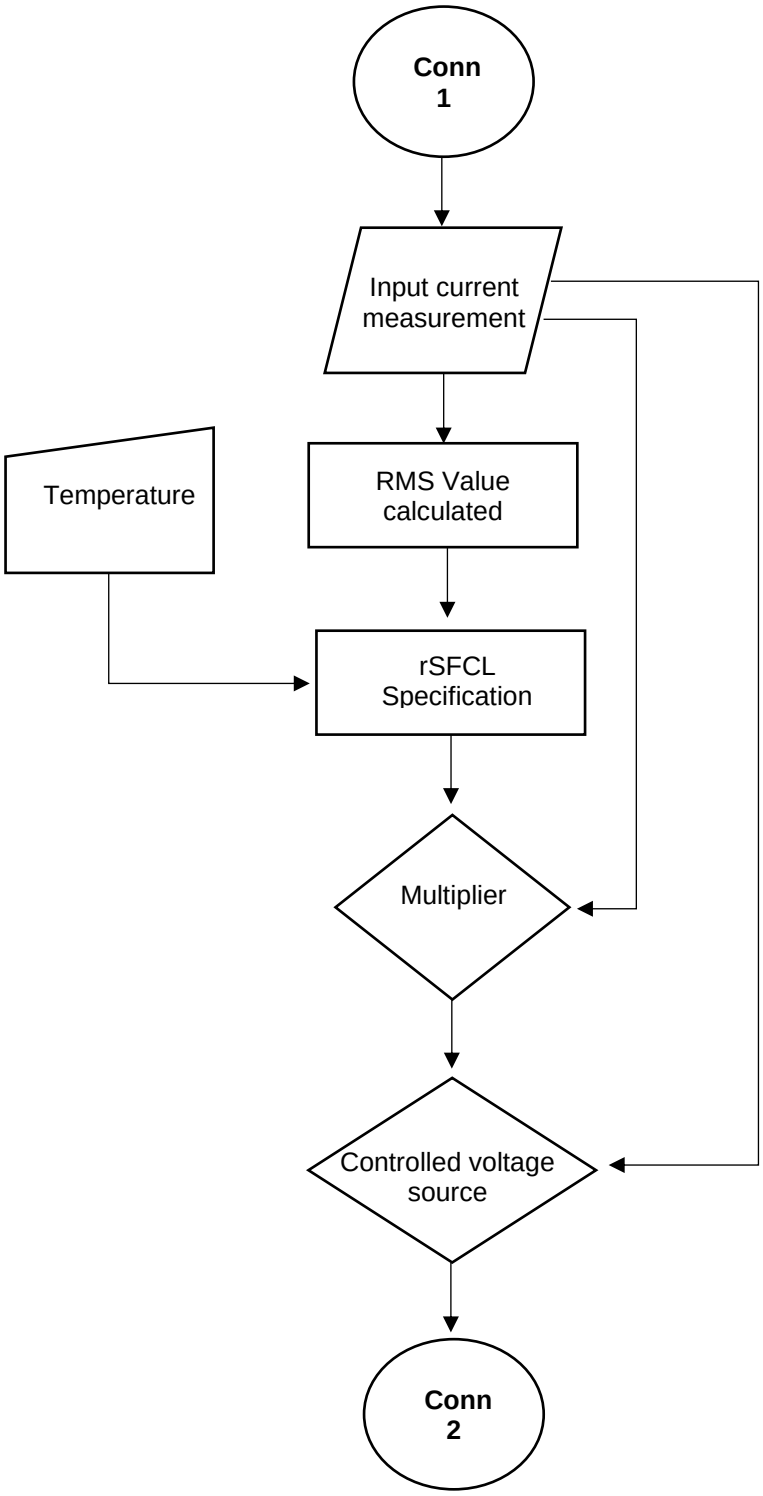

Fig. 3. 11: rSFCL model flowchart

Table 6 shows fundamental parameters of the simulation model. It is important to note the six different parameters, description, and values as they are a summary of the model specifications.

Table 6: Fundamental parameters for the rSFCL design and simulation.

Parameters	Description	Values
The transition time	The time it takes for rSFCL to switch from superconducting state fault current limiting state.	2 ms
The minimum resistance	The resistance magnitude of the rSFCL during superconducting state	0.01 Ω
The maximum resistance	The resistance of the rSFCL under a SCC (Fault current limiting state). It's also known as the quench state.	50 Ω
The operating current	The magnitude of current required to initiate quenching.	200 A
The recovery time	The time taken after a short circuit has been cleared and the rSFCL is switching from quenching state back to superconducting state.	10 ms
The critical temperature	The temperature in which the SFCL will initiate quenching at.	77 K

3.6.2 Simulation of rSFCL model

The MATLAB Simulink model shown in Fig. 3. 9 is only capable to limit fault current on a single phase, therefore in a three-phase network a similar model must be duplicated to the other two phases. In most cases, when a fault occurs in a three-phase system the current becomes unbalance and the rSFCL of each phase will be triggered separately by a current flowing in individual phase. With such an imbalance of current between phase currents, quenching might be initiated in one or two phases, therefore it is vital for each phase to have its own rSFCL installed to achieve accurate quenching (Zhang, 2017).

The following are different scenarios that were simulated based on the prototype shown in Fig. 3. 9.

3.6.2.1 SCENARIO 1: FCL model under normal operation

Fig. 3. 12 illustrates a schematic diagram of an operational simulation model of rSFCL. The difference between Fig. 3. 9 and Fig. 3. 12 is that Fig. 3. 12 has an AC current source used to simulate the input current and scopes that are used to display measurements of

input current, RMS current, Temperature, and control voltage. The main purpose of this model was to demonstrate the change in control signal of the CVS when “I” and “T” are below critical current of 200 A and critical temperature of 77 K respectively. The AC current source is set to inject 100 A and the temperature is set to 50 K. The waveforms for input current and RMS current before a fault occurs is shown in Fig. 3. 13. Furthermore, Fig. 3. 14 and Fig. 3. 15 demonstrate the wave form of control voltage and input temperature respectively.

The purpose of this scenario is to find waveforms that will be used as a reference to study the change in current and voltage after critical current and temperature has been reached.

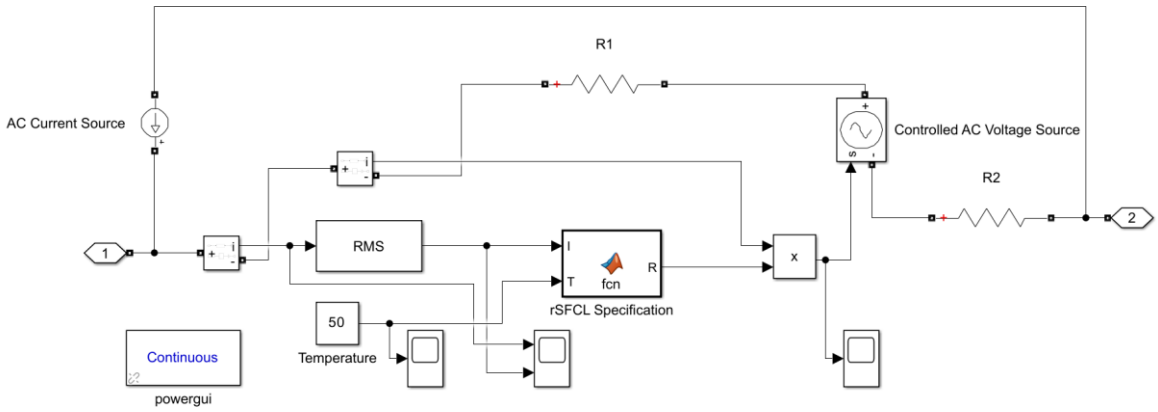

Fig. 3. 12: Operational MATLAB Simulink Schematic diagram.

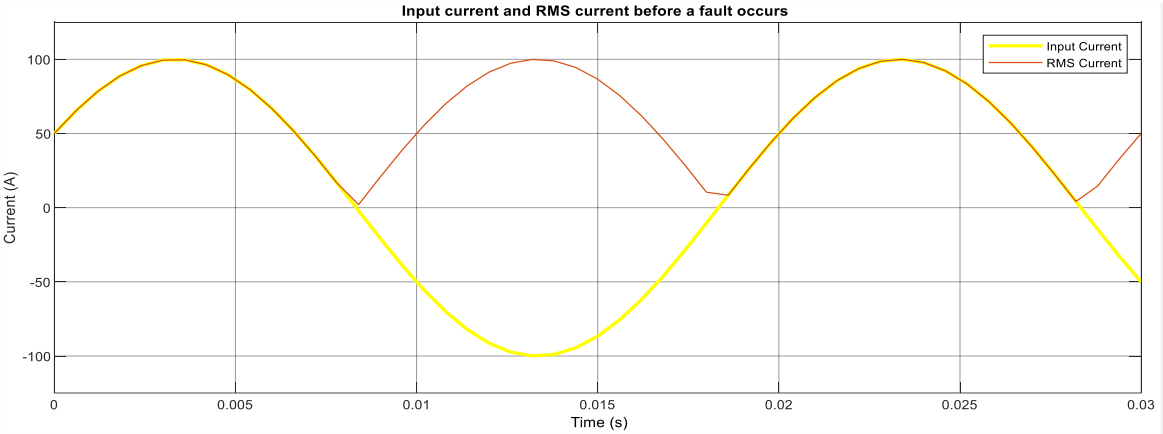

Fig. 3. 13: Input current and RMS current before a fault occurs.

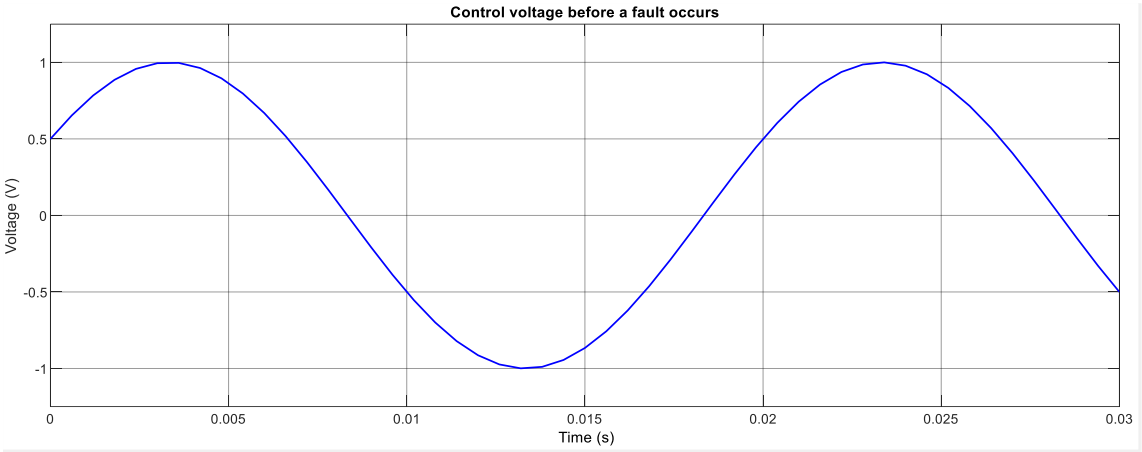

Fig. 3. 14: Control voltage before a fault occurs

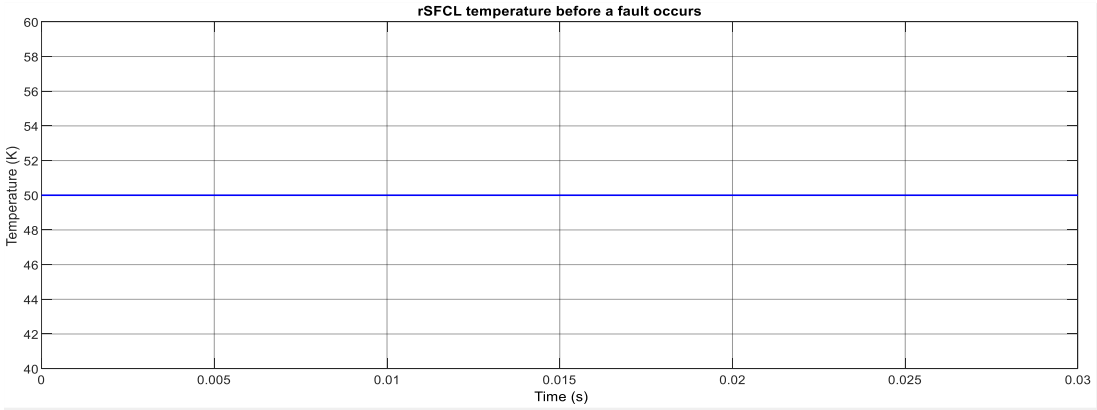

Fig. 3. 15: rSFCL temperature before a fault occurs

3.6.2.2 SCENARIO 2: FCL model with fault current and temperature above set point

The purpose of this scenario is to show the change in current and voltage waveform when the model operates above critical values. The AC current source is set to inject 400 A to simulate a fault condition as demonstrated in Fig. 3. 17. The RMS current is also shown on the same plot. A control voltage waveform is shown in Fig. 3. 18. This waveform must be looked at with reference to the waveform shown in Fig. 3. 14 to determine the effect caused by rSFCL function block. It is observed that the peak value of control voltage has increased from 1 V to 20 kV. Fig. 3. 19 shows a temperature waveform set to 80 K.

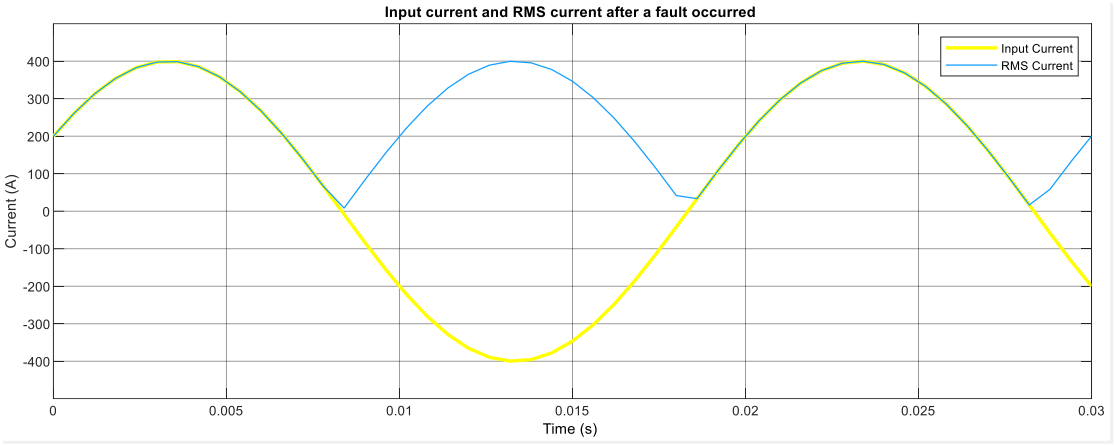

Fig. 3. 16: Input current and RMS current after a fault occurred

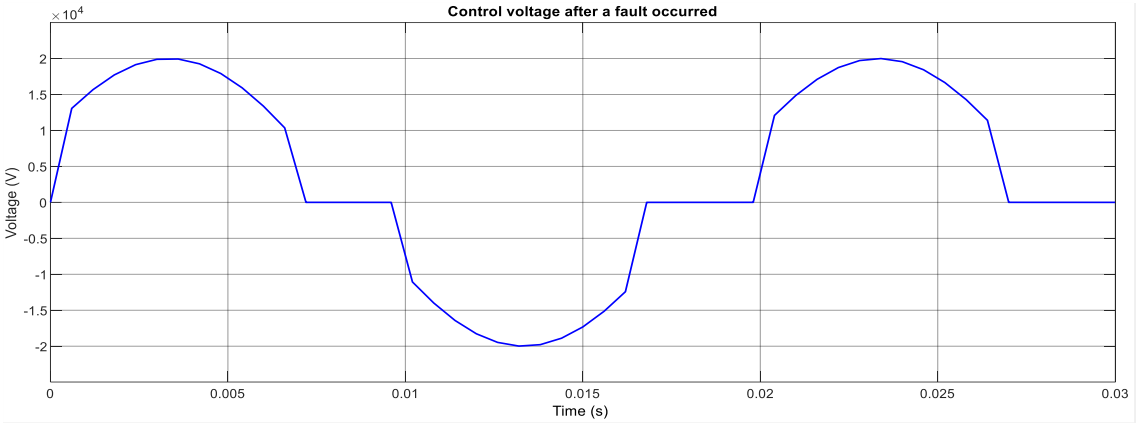

Fig. 3. 17: Control voltage after a fault occurred

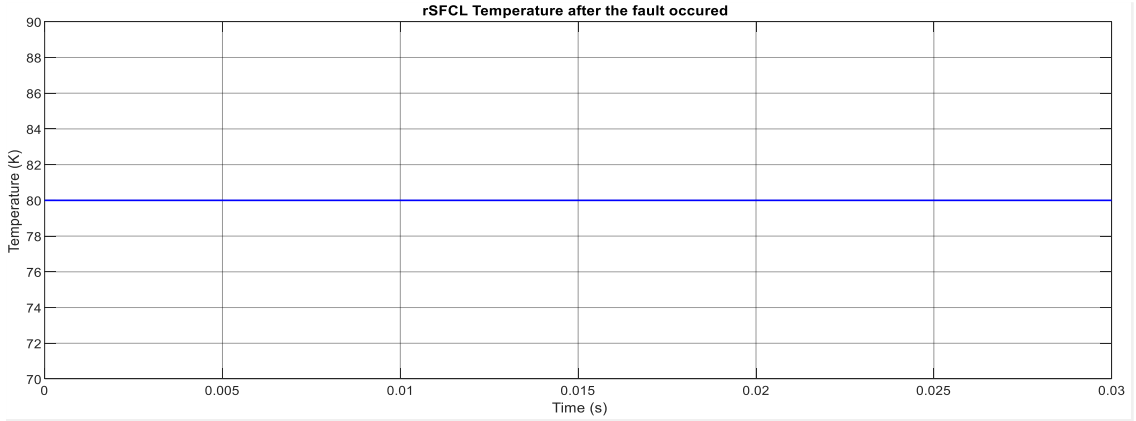

Fig. 3. 18: rSFCL temperature after a fault occurred

3.6.2.3 SCENARIO 3: IEEE 9 bus power system model under normal operation

Fig. 3. 19 demonstrate an IEEE 9 Bus system that was used to test the impact of rSFCL model when it is integrated to a real-life power system. Location 1 & 2 of the rSFCL model and Location 1 & 2 of the Fault has also been indicated on the diagram to make it easy to reference during the discussions.

In this scenario, the IEEE 9 bus system was simulated without a rSFCL model and Fault being introduced into the system. The purpose of this scenario is to obtain reference waveforms of three phase current from Bus_1, Bus_2, Bus_3, Bus_5, Bus_6, and Bus_8 when the power system is operating under-normal condition.

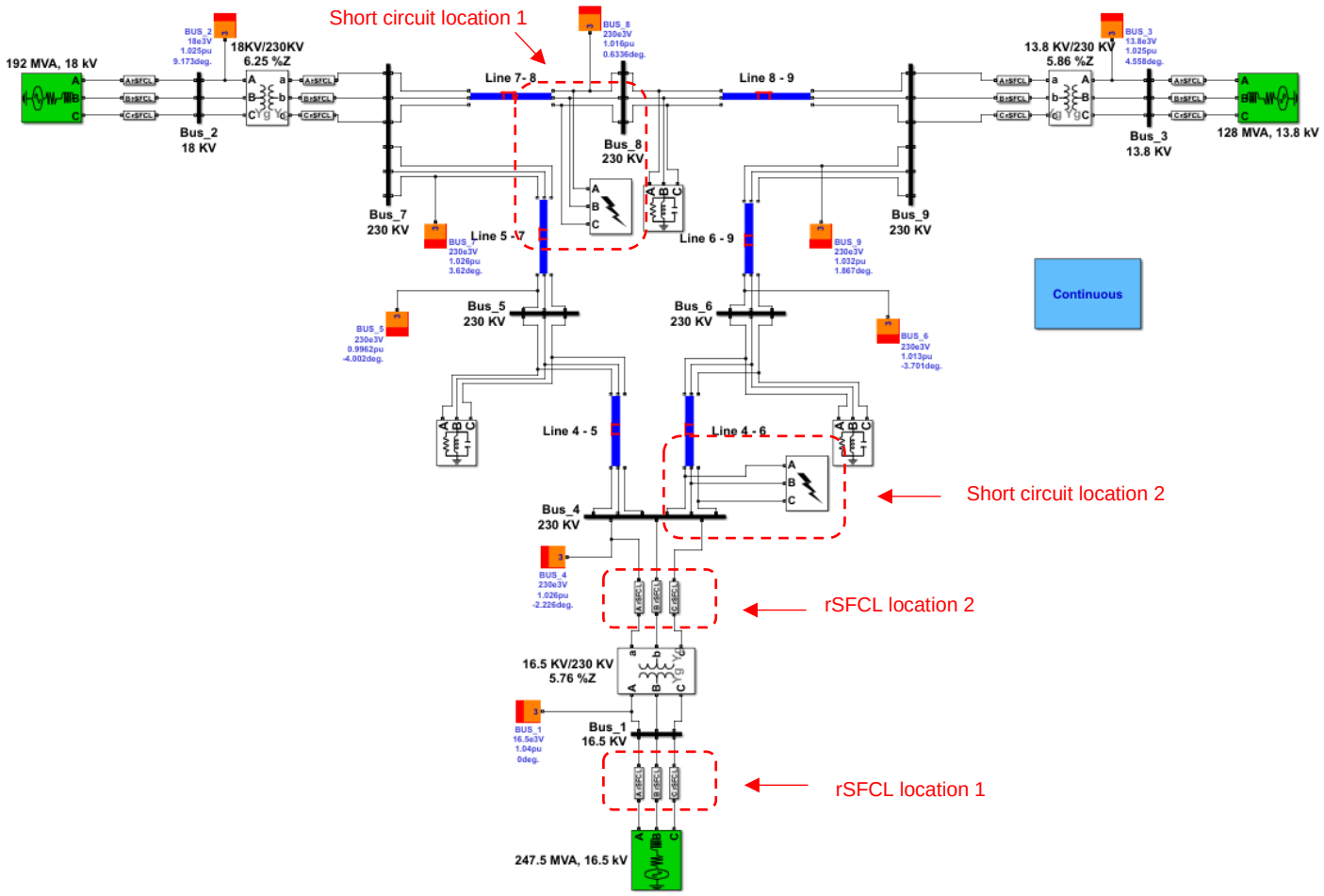

Fig. 3. 19: IEEE 9 Bus system with rSFCL and a Short Circuit simulation

Fig. 3. 20 shows the three phase current wave forms measured in Bus_1, Bus_2, Bus_3, Bus_5, Bus_6, and Bus_8. These values were obtained without the rSFCL and Fault being introduced into the system.

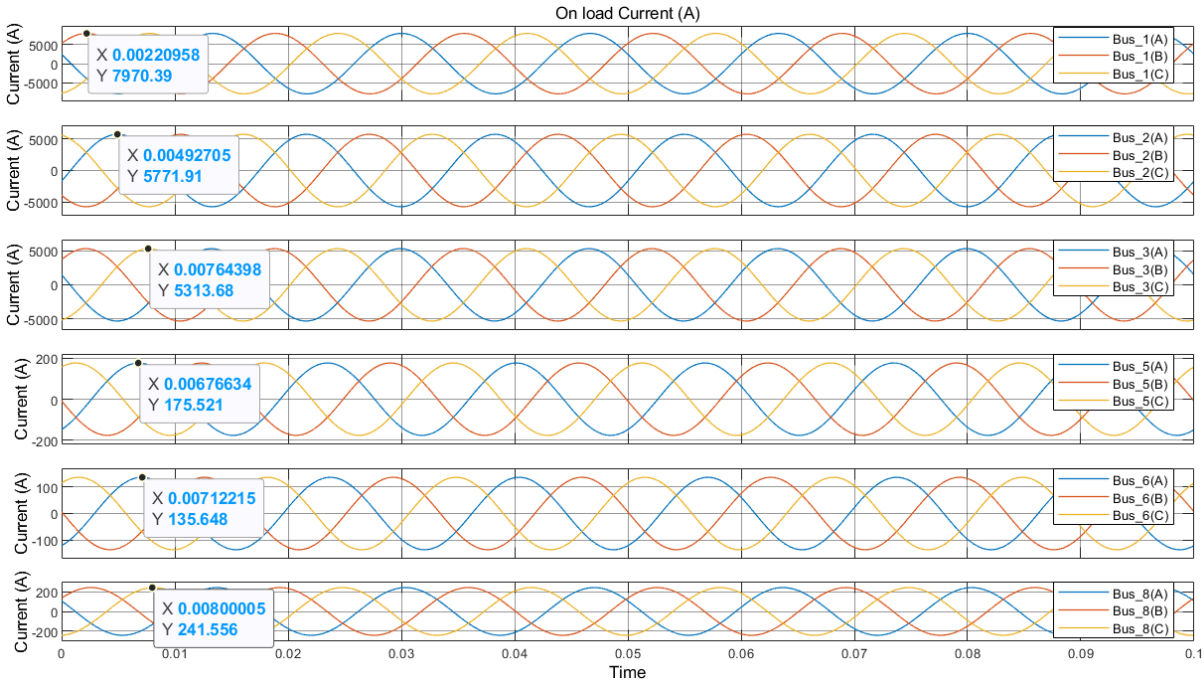

Fig. 3. 20: Three phase current wave forms measured in Bus_1, Bus_2, Bus_3, Bus_5, Bus_6, and Bus_8 when operating under normal condition.

3.6.2.4 SCENARIO 4: IEEE 9 bus power system model with a short circuit in short circuit location 1

In this scenario, the rSFCL was removed and a short circuit was simulated at Short Circuit location 1 as demonstrated in Fig. 3. 19. The purpose of this scenario was to obtain benchmark SCC measurements. These benchmarked SCC measurements would be compared with SCC measurements obtained when the rSFCL is operating at quenching state. Quenching state is a state at which the rSFCL is expected to add large impedance into the power system to limit fault current. The absence of rSFCL in this in Fig. 3. 19 is equivalent to rSFCL operating at superconducting state.

The parameters of the SC are as follows:

- Switching time – [0.005 – 0.03]
- Fault resistance – 0.001 Ω
- Ground resistance – 0.01 Ω
- Snubber resistance – 1e6 Ω

Fig. 3. 21 shows the three phase current wave forms measured in Bus_1, Bus_2, Bus_3, Bus_5, Bus_6, and Bus_8. These values were obtained after a Fault was introduced however, without the rSFCL being included into the system.

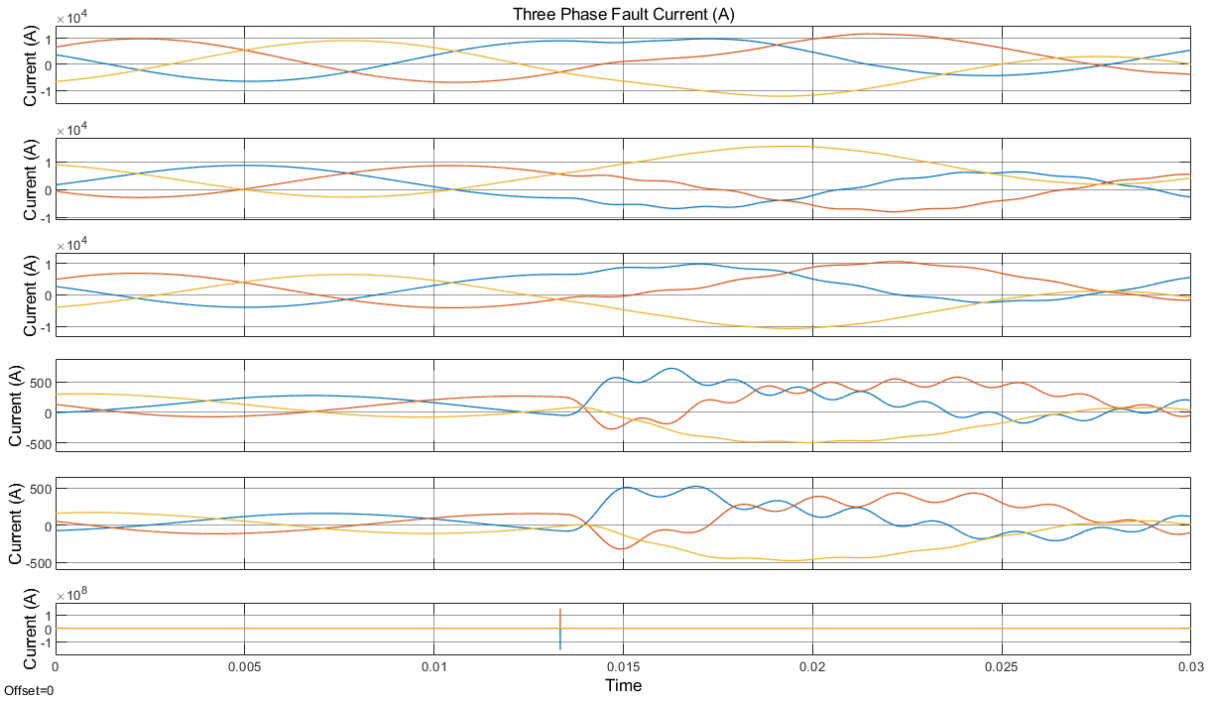

Fig. 3. 21: Three phase current wave forms measured in Bus_1, Bus_2, Bus_3, Bus_5, Bus_6, and Bus_8 with a fault simulated of Fault Location 1

3.6.2.5 SCENARIO 5: IEEE 9 bus power system model with rSFCL installed in location 1 and a SC in location 1 (current and temperature above pick up)

In this scenario, rSFCL model was installed in rSFCL location 1 and a Short Circuit condition was simulated in short circuit location 1 as demonstrated in Fig. 3. 19. The purpose of this scenario was to study the impact caused by rSFCL to the three-phase peak SCC magnitude. The rSFCL was expected to significantly reduce the SCC magnitude as it was operating at quenching state in this scenario.

- **Added unit delay**

In this scenario, the rSFCL model was modified and a unit delay was added to avoid algebraic loops as demonstrated in Fig. 3. 22. An algebraic loop usually occurs when there is a loop between the input and output signal with only direct feedthrough blocks. Direct feedthrough is when the block output is controlled by the value of signal coming through input connection port, and the value of the input connection port depends on the value of the output.

For example, the output of the controlled voltage source in rSFCL model as shown in Fig. 3. 22 depends on the current of the system coming through connection port 1, and in the meantime the current of the system is affected by the voltage output of the rSFCL model. Therefore, an effective way to eliminate the algebraic loop was to introduce a non-direct-feedthrough block such as the Unit Delay (Zhang, 2017).

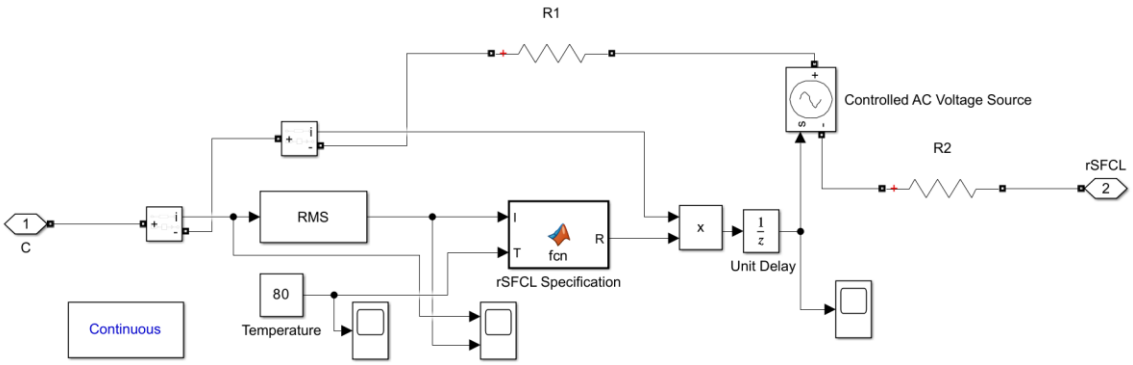

Fig. 3. 22: MATLAB Simulink schematic diagram of a rSFCL model with a unit delay added.

- **Function block**

In this scenario the function block algorithm was also adjusted to suit the SCC levels of different buses where the rSFCL model was located as demonstrated in Fig. 3. 19.

The peak nominal current that was flowing at Bus_1, Bus_2, and Bus_3 was measured to be 7.970 kA, 5.771 kA, and 5.313 kA respectively. Therefore, the critical current settings for the three function block algorithms were respectively set to 8 kA, 6 kA, and 5.5 kA as demonstrated in Fig. 3. 23, Fig 3. 24, and Fig 3. 25. These settings are only applicable to these specific rFCL location, the critical current setting would have tobe adjusted in line with the changes on the system. The critical temperature was set to 77 K.

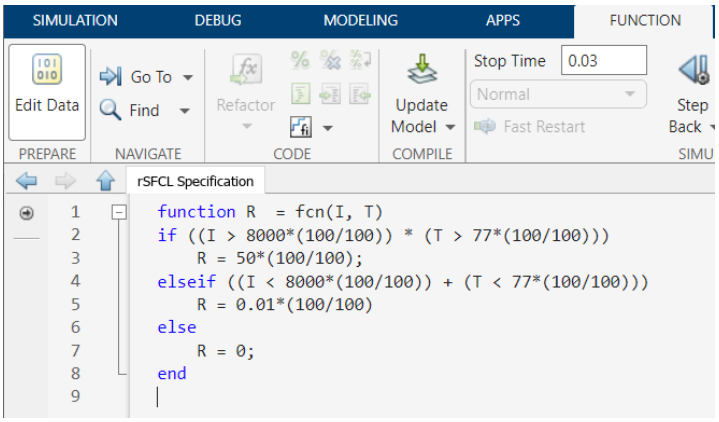

Fig. 3. 23: Function block algorithm of rSFCL model at Bus_1

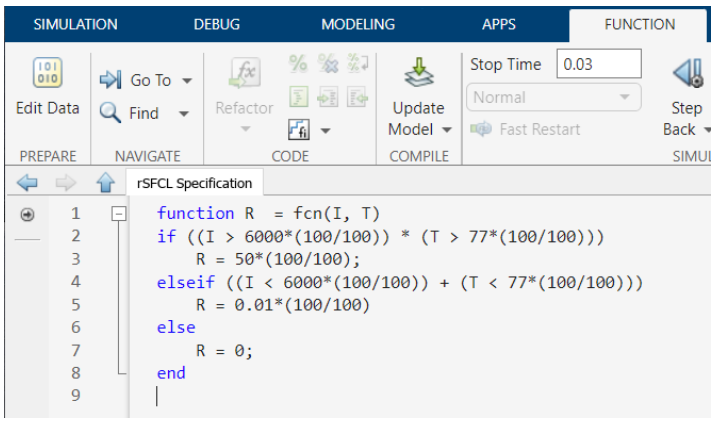

Fig. 3. 24: Function block algorithm of rSFCL model at Bus_2

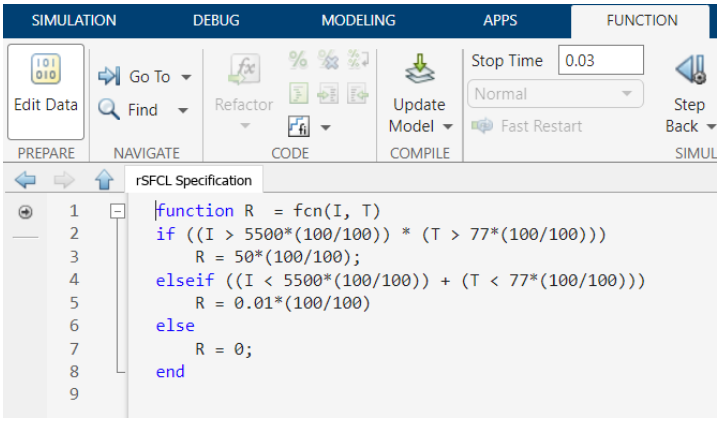

Fig. 3. 25: Function block algorithm of rSFCL model at Bus_3

- **Simulation**

Due to the SC condition the critical current of rSFCL was exceeded and the temperature input was set to 80 K. Under such conditions the rSFCL switched from superconducting state to quenching state. Fig. 3. 26 demonstrate the Three phase current wave forms measured in Bus_1, Bus_2, Bus_3, Bus_5, Bus_6, and Bus_8 with a rSFCL model installed at rSFCL location 1 and a fault simulated of Fault Location 1.

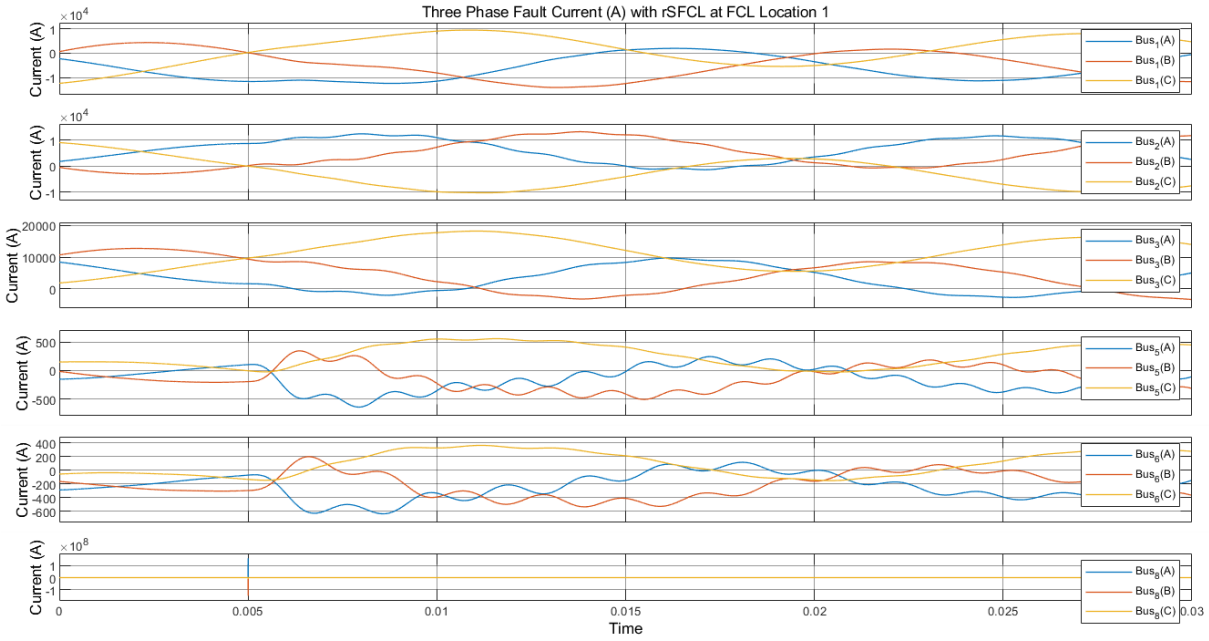

Fig. 3. 26: Three phase current wave forms measured in Bus_1, Bus_2, Bus_3, Bus_5, Bus_6, and Bus_8 with a rSFCL model installed at rSFCL location 1 and a fault simulated of Fault Location 1

3.6.2.6 SCENARIO 6: IEEE 9 bus power system model with rSFCL installed in location 1 and a short circuit in location 2 (current and temperature above pick up)

In this scenario, the rSFCL was installed in location 1 and a short circuit at location 2. The purpose of this scenario was to assess the change in current measurement when the location of the short circuit has been changed. Fig. 3. 27 shows the current measurements when the power system is operating under such conditions.

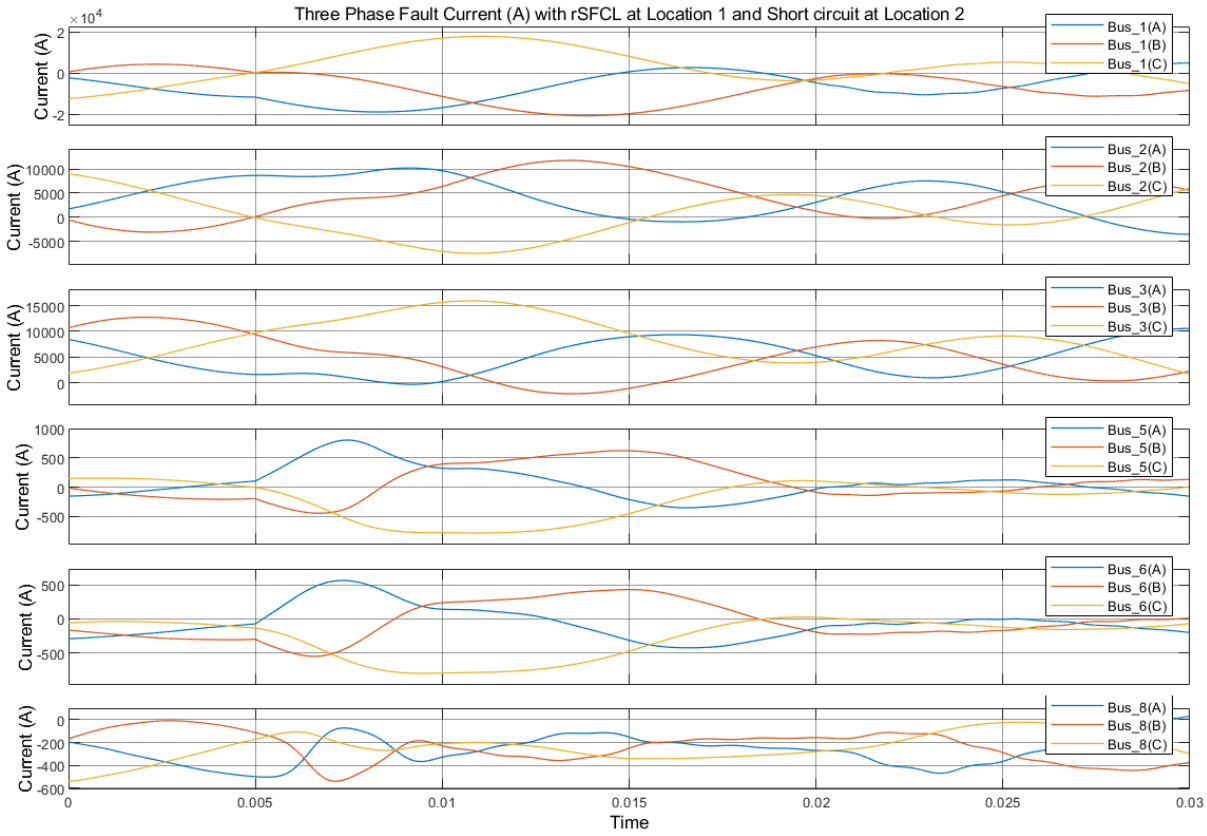

Fig. 3. 27: Three phase current wave forms measured in Bus_1, Bus_2, Bus_3, Bus_5, Bus_6, and Bus_8 with a rSFCL model installed at rSFCL location 1 and a fault simulated of Fault Location 2

3.6.2.7 SCENARIO 7: IEEE 9 bus power system model with rSFCL installed in location 2 and a short circuit in location 1 (current and temperature above pick up)

In this scenario, the rSFCL was installed at rSFCL location 2 and a short circuit simulated at short circuit location 1. The purpose of this scenario was to observe the effect that the change of short circuit location will have towards the currents measured in different buses. Fig. 3. 27 shows the three phase current wave forms measured in Bus_1, Bus_2, Bus_3, Bus_5, Bus_6, and Bus_8.

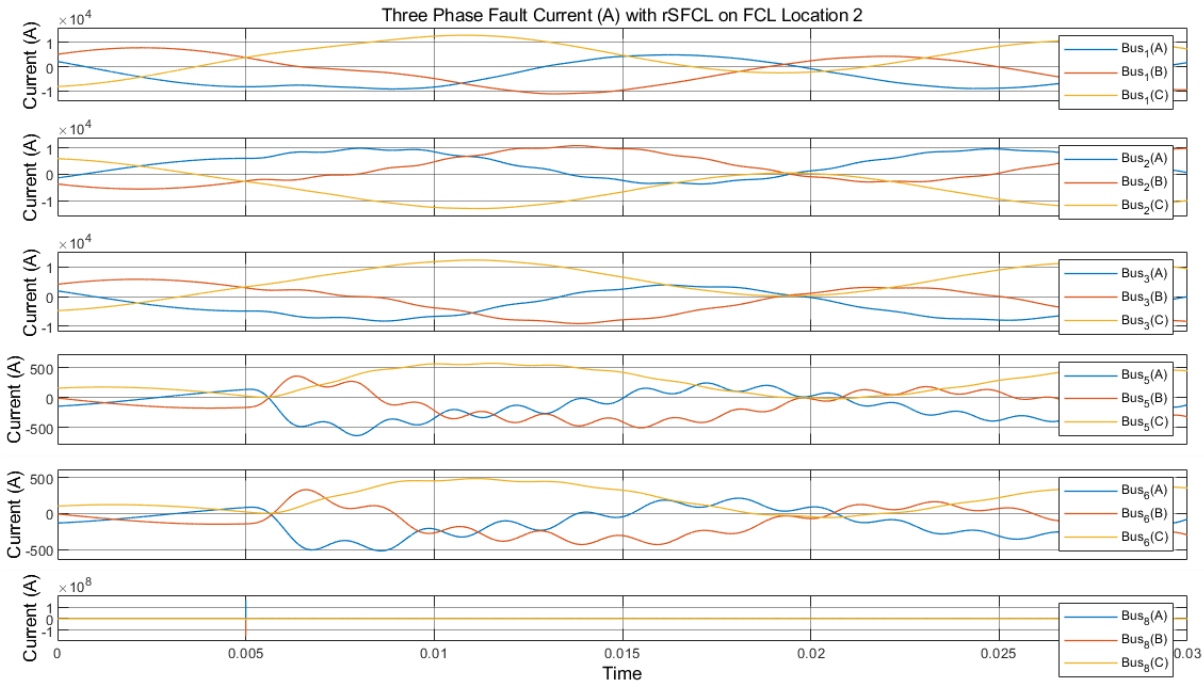

Fig. 3. 28: Three phase current wave forms measured in Bus_1, Bus_2, Bus_3, Bus_5, Bus_6, and Bus_8 with a rSFCL model installed at rSFCL location 2 and a fault simulated of Fault Location 1

3.6.2.8 SCENARIO 8: IEEE 9 bus Power system model with rSFCL operating at quenching mode and optimal resistance increased by 20% (current and temperature above pick up)

In this scenario, the power system network was arranged as demonstrated in scenario 5. However, the function block algorithm was changed and programmed as shown in Fig. 3. 29. In this case the optimal resistance (50 Ω) was increased by 20% to simulate a situation where there has been an expansion of the network and the impedance of the grid has increased and the rSFCL need to adjust accordingly. The percentage at which the optimal resistance is increased is directly proportional to the percentage at which the grid impedance has increased.

When the grid impedance increase, the peak value of SCC decreases that is measured on the busbars. The decreased SCC could affect the operation of protection devices since their settings are calculated based on specific value of SCC.

Therefore, the optimal resistance must be increased so that more current is limited. When the SCC flowing in the primary winding is decreased, the SCC on the secondary winding will be increased to keep accommodating the increased grid impedance and maintain an adequate SCC magnitude. Maintaining an adequate SCC is important to avoid having to adjust protection settings in IEDs.

Fig. 3. 29 demonstrate a function block algorithm where the optimal resistance was increased by 20 %.

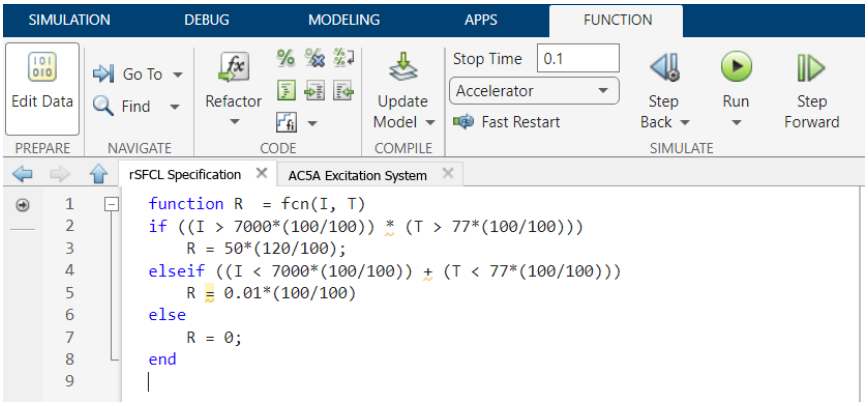

Fig. 3. 29: Function block algorithm of the rSFCL with Optimum shunt resistance increased by 20 %

3.6.2.9 SCENARIO 9: IEEE 9 bus Power system model with rSFCL operating at quenching mode and optimum resistance decreased by 20% (current and temperature above pick up)

In this scenario, the power system network was also arranged as demonstrated in scenario 5 however, the function block algorithm was also changed and programmed as shown in Fig. 3. 30. In this case the optimum shunt resistance (50 Ω) was decreased by 20% to simulate a condition where the number of generation sources have increased in the network and the rSFCL need to adjust accordingly. The percentage at which the optimal resistance is decreased is directly proportional to the percentage at which the generation sources have increased.

When the number of generation sources increase in the network, the peak value of fault current also increases. Therefore, a decrease of the optimal resistance is required to maintain an adequate SCC. When the optimal resistance is decrease that will result into less fault current being limited in the primary winding of the transformer meaning fault currents will me high in that side of the winding. When the current is high on the primary winding then it means it will be less on the secondary winding.

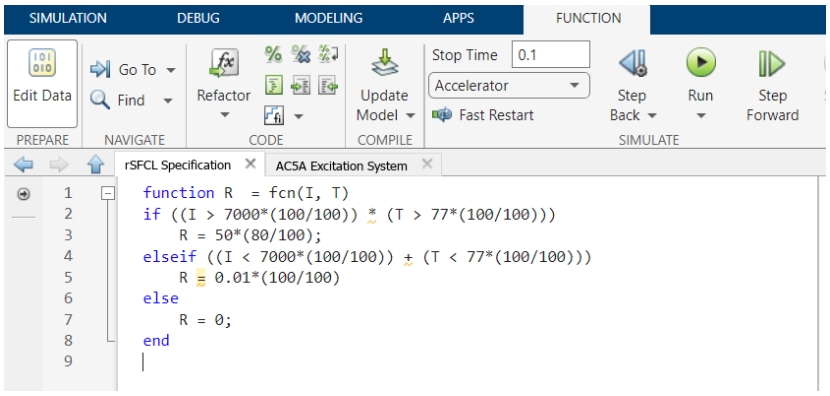

Fig. 3. 30 Function block algorithm of the rSFCL Optimum resistance decreased by 20%

3.7 Summary

This chapter has covered the mathematical representation of periodic and aperiodic components of SCC, where the components of a current before and after a short circuit has occurred were proven to not be the same. The mathematical representation of a SCC on a simplified power system was also discussed, where the mathematical expressions of that proves that during a fault current the load impedance is ignored. Only the source and fault impedance are considered to derive the line current. Furthermore, The E-J characteristic and determination of optimum shunt reactance was discussed, where mathematical expressions of different regions/zones of the HTS such as superconducting zone, flux zone, and normal zone were derived.

Furthermore, this chapter has covered, a rSFCL model that consist of a controlled voltage source that is equivalent to a variable resistor and a function block that with an algorithm that monitors the input current and temperature was built. The model has specifications such as critical current set to 200 A and critical temperature set to 77 K. A simulation was done and waveforms that represent the control voltage before and after a critical temperature is reached was obtained. The control voltage is observed to have been significantly increased after a critical current and temperature has been reached.

The rSFCL was integrated into an IEEE 9 bus power system, where different scenarios such as different locations of rSFCL and different locations of short circuits were simulated. It is important to include a unit delay in the rSFCL model to avoid algebraic loops. Through increasing or decreasing the optimum shunt resistance, the level of SCC quenched can be controlled when changes occur in the network, such as increase in number of generation sources or expansion of the power system from the load side.

CHAPTER 4: Results and discussion

4.1 Introduction

In this chapter, the simulation results of different scenarios that were simulated in chapter 3 where the rSFCL model is integrated to an IEEE 9 bus power system model is analysed and discussed into detail. Scenario 4 is compared with scenario 5, scenario 5 with scenario 6, and scenario 5 with scenario 7.

4.2 Results of scenario 4 and scenario 5

Scenario 4 represent the IEEE 9 bus power system model with a short circuit in short circuit location 1, and Scenario 5 represent the IEEE 9 bus power system model with rSFCL installed in rSFCL Location 1 and a short circuit in short circuit Location 1 (current and temperature above pick up). Table 7 demonstrates the peak values of the three phase current wave forms that were obtained from the two scenarios.

It is important to note that during the simulation of scenario 5 the rSFCLs that are located near bus_1 ware operating at quenching state and the rSFCLs that were located near bus_2 and bus_3 was operating at superconducting state. It is therefore, observed that the rSFCL model at phase C which measured the highest peak values has reduced the SCC by approximately 27.05%. This can be considered to be a reduction that is significant enough to eliminate excessive SCC.

Bus_5, Bus_6, and Bus_8 had also measured significant enough drop of the highest peak when the rSFCL was operating at quenching mode with Bus_6 reduced by 26.32%

Table 7: Data analysis and Comparison for scenario 4 and scenario 5

Scenario 4 and 5				
Bus	**Scenario**	**Phase A (kA)**	**Phase B (kA)**	**Phase C (kA)**
1	4	5045	7971	13080
1	5	1995	4390	9541
% Difference		-60.45%	-44.92%	-27.05%
2	4	9592	10600	290
2	5	12360	13180	2936
% Difference		28.85%	24.33%	912.41%
3	4	3502	5315	11850
3	5	9713	1274	18210
% Difference		177.35%	-76.03%	53.67%
5	4	243.3	359.3	573.9

5	5	243.9	345.1	558.8
% Difference		0.24%	-3.95%	-2.63%
6	4	221.4	341.7	496.5
6	5	117	199.7	365.8
% Difference		-47.15%	-41.55%	-26.32%
8	4	160300000	241.8	239.7
8	5	159200000	-8.5	-170.6
% Difference		-0.68%	-103.51%	-171.17%

4.3 Results of scenario 5 and scenario 6

Scenario 5 represent the IEEE 9 bus power system model with rSFCL installed in rSFCL Location 1 and a short circuit in short circuit Location 1 (current and temperature above pick up). Scenario 6 represent the IEEE 9 bus power system model with rSFCL installed in location 1 and a short circuit in location 2 (current and temperature above pick up). Table 8 demonstrates the comparison of these two scenarios. Short circuit location 1 is situated at a location that is far from bus_1 rSFCL and short circuit location 2 is situated at a location that is near. Bus_1 is used as a reference in this case because it is a bus that is operating at quenching state.

The peak SCC measurements of bus_1, phase C, scenario 5 shows that the SCC was reduced to 9.54 kA and the peak SCC measurements of bus_1, phase C, scenario 6 shows that the SCC was reduced to 12.85 kA. That is a difference of 34.68% which is considered to be a significant difference. Therefore, it is concluded that the location of the short circuit does have an impact on the magnitude at which the SCC is reduce. The levels of SCC increase when the short circuit occurs closer to the source and that affects the margins at which the rSFCL reduce the SCC.

Table 8: Data analysis and Comparison for scenario 5 and scenario 6

Scenario 5 and 6				
Bus	**Scenario**	**Phase A (kA)**	**Phase B (kA)**	**Phase C (kA)**
1	5	1995	4390	9541
1	6	4831	7747	12850
% Difference		142.15%	76.469248	34.681899
2	5	12360	13180	2936
2	6	9801	10790	477.1

% Difference		-20.703883	-18.133536	-83.75
3	5	9713	1274	18210
3	6	3917	5813	12290
% Difference		-59.672604	356.27943	-32.50961
5	5	243.9	345.1	558.8
5	6	243.9	359.5	573.9
% Difference		0	4.1727036	2.702219
6	5	117	199.7	365.8
6	6	214.5	332.9	488.2
% Difference		83.333333	66.70005	33.460908
8	5	159200000	-8.5	-170.6
8	6	160200000	100600	72.64
% Difference		0.6281407	-1183629.4	-142.57913

4.4 Results of scenario 5 and scenario 7

Scenario 5 represent the IEEE 9 bus power system model with rSFCL installed in rSFCL Location 1 and a short circuit in short circuit Location 1 (current and temperature above pick up). Scenario 7 represent the IEEE 9 bus power system model with rSFCL installed in location 2 and a short circuit in location 1 (current and temperature above pick up). Table 9 demonstrates the peak values of the three phase current wave forms that were obtained from the two scenarios.

The peak SCC measurements of bus_1, phase C, scenario 5 shows that the SCC was reduced to 9.54 kA and the peak SCC measurements of bus_1, phase C, scenario 7 shows that the SCC was reduced to 17.99 kA. That is a difference of 88.5 % which is a much more significant difference. Therefore, it is concluded that the rSFCLs are more efficient when they are located closer to the source.

Table 9: Data analysis and Comparison for scenario 5 and scenario 7

Scenario 5 and 7				
Bus	**Scenario**	**Phase A (kA)**	**Phase B (kA)**	**Phase C (kA)**
1	5	1995	4390	9541
1	7	5000	4390	17990
% Difference		150.62 %	0 %	88.55 %
2	5	12360	13180	2936

2	7	10190	11760	4706
% Difference		-17.55 %	-10.77 %	60.28 %
3	5	9713	1274	18210
3	7	9354	12740	15950
% Difference		-3.69 %	900 %	-12.41 %
5	5	243.9	345.1	558.8
5	7	803.2	623.9	152.8
% Difference		229.31 %	80.78 &	-72.65 %
6	5	117	199.7	365.8
6	7	564.6	431.2	28.85
% Difference		382.56 %	115.92 %	-92.11 %
8	5	159200000	-8.5	-170.6
8	7	-72.93	-8.4	-21.42
% Difference		-100.00 %	-1.17 %	-87.44 %

4.5 Summary

This chapter has covered the data analysis and comparison of scenario 4, 5, 6, and 7. The data shows that the rSFCL model does reduce the SCC levels when located at an efficient location such as close to the source of current. The measurements indicates that the peak value of the three current at bus_1 is reduced by approximately 27.05 %.

CHAPTER 5: Conclusion

The literature on impact of bulk penetration of RES to the fault current levels of the system, distributed energy sources, theory of fault currents, different strategies and technologies were studied through chapter two. FCL were identified to be an adequate technology to reduce excessive power system Short Circuit currents. With many different types of fault current limiters, including but not limited to Superconducting FCL, Solid-state FCL, hybrid FCL, etc. The Resistive superconductive fault current limiter(rSFCL) was further systematically identified to be a better emerging technology with manageable drawbacks. A MATLAB Simulink model for the rSFCL was designed and simulated. In this model-controlled voltage source, equivalent to variable resistor was used to reduce the fault currents in the power system model. The designed rSFCL model was further integrated to an IEEE 9 bus power system to study how the network behaves to a three phase to ground short circuit with and without the quenching resister. The results shows that indeed the rSFCL does reduce the fault currents by a significant margin.

Recommendations

Grid owners need to monitor the SCC levels of their grid in reference to the SCC rating of the installed apparatus. For each application of FCL, the different FCL devices must be explored to ensure adequate fit for any chosen technology. The design of the FCL should be flexible enough to accommodate future changes on the network such as the change in configuration of the grid or grid expansion.

Future work

FCL control strategies shall be the area of focus as grid codes require fault ride through capabilities for all inverter-based RES. The FCL control strategies have a potential to eliminate some of the drawbacks that are presented by rSFCL such as inability to limit the first wave of the fault currents. In some instances, the presence of the first wave might be significant enough to cause devastating effects to the system apparatus.

REFERENCES

Adnan, A.Z., Yusoff, M.E. & Hashim, H. 2018. Analysis on the impact of renewable energy to power system fault level. *Indonesian Journal of Electrical Engineering and Computer Science*, 11(2): 652–657.

Alam, M.S., Abido, M.A.Y. & El-Amin, I. 2018. Fault current limiters in power systems: A comprehensive review. *Energies*, 11(5).

Anon. 2020. Electricity Market Report. *Electricity Market Report*.

Anon. 2023. Historic Daily Peak System Capacity/Demand. , 12(2002): 1–5.

Anon. 2012. Hydroelectric Power. *Investing in Energy*: 145–152.

Asghar, R. 2018. Fault Current Limiters Types, Operations and its limitations. *International Journal of Scientific & Engineering Research*, 9(2): 1020–1027. http://www.ijser.org.

Buraimoh, E. & Davidson, I.E. 2020. Overview of Fault Ride-Through Requirements for Photovoltaic Grid Integration, Design and Grid Code Compliance. *9th International Conference on Renewable Energy Research and Applications, ICRERA 2020*: 332–336.

Chetty, V. 2016. NETWORK STUDIES AND MITIGATION OF HIGH 132 kV FAULT CURRENTS IN ETHEKWINI ELECTRICITY. , (December). https://researchspace.ukzn.ac.za/xmlui/bitstream/handle/10413/14980/Chetty_Vasudevan_2016.pdf?sequence=1&isAllowed=y.

Chetty, V., Davidson, I.E. & Sharma, G. 2021. The Recent Trend of Increasing Fault Current Levels and Mitigation Measures. *2021 Southern African Universities Power Engineering Conference/Robotics and Mechatronics/Pattern Recognition Association of South Africa, SAUPEC/RobMech/PRASA 2021*.

Demin, S., Sitbon, M., Aharon, I., Barbi, E., Machlev, R., Belikov, J., Levron, Y. & Baimel, D. 2023. A new resonant fault current limiter for improved wind turbine transient stability. *Electric Power Systems Research*, 223(June).

Eckroad, S. 2009. Superconducting Fault Current Limiters EPRI Project Manager. *Superconducting Fault Current Limiters Technology Watch 2009* . https://www.suptech.com/pdf_products/faultcurrentlimiters.pdf.

Endo, M., Hori, T., Koyama, K., Yamaguchi, I., Arai, K., Kaiho, K. & Yanabu, S. 2008. Operating characteristics of superconducting fault current limiter using 24kV vacuum interrupter driven by electromagnetic repulsion switch. *Journal of Physics: Conference Series*, 97(1): 3–8.

Eyuboglu, O.H., Dindar, B. & Gul, O. 2020. Series Resonance Type Fault Current Limiter for Fault Current Limitation and Voltage Sag Mitigation in Electrical Distribution Network. *Proceedings - 2020 IEEE 2nd Global Power, Energy and Communication Conference, GPECOM 2020*: 256–261.

Fang, H., Li, Z., Zhang, X. & Xiong, J. 2023. Fault current limitation control of multiple distributed renewable generations under unbalanced conditions. *Energy Reports*, 9: 221–229.

Gabr, M.A., Megahed, T.F. & Abdelkader, S.M. 2021. Fault Current Management Under High Penetration of Distributed Generation in Smart Grids. : 106–111.

Gers, J.M. & Holmes, E. 2021. Calculation of short circuit currents. *Protection of Electricity*

Distribution Networks, (158): 11–41.

Gonçalves Sotelo, G., Santos, G. dos, Sass, F., França, B.W., Nogueira Dias, D.H., Zamboti Fortes, M., Polasek, A. & de Andrade Jr., R. 2022. A review of superconducting fault current limiters compared with other proven technologies. *Superconductivity*, 3: 100018.

Guillen, D., Salas, C., Trillaud, F., Castro, L.M., Queiroz, A.T. & Sotelo, G.G. 2020. Impact of Resistive Superconducting Fault Current Limiter and Distributed Generation on Fault Location in Distribution Networks. *Electric Power Systems Research*, 186(March): 106419. https://doi.org/10.1016/j.epsr.2020.106419.

Gumilar, L., Afandi, A.N., Aripriharta, A. & Rahmawati, Y. 2020. Reduction of short circuit current fault on photovoltaic and wind power plant as distributed generation using sfcl. *EECCIS 2020 - 2020 10th Electrical Power, Electronics, Communications, Controls, and Informatics Seminar*: 9–14.

Guo, Y., Huang, C. & Zhao, J. 2020. Resonance Type Superconducting Fault Current Limiters: Theory and Applications. *2020 IEEE International Conference on Applied Superconductivity and Electromagnetic Devices, ASEMD 2020*: 16–17.

Hooshyar, H., Heydari, H., Savaghebi, M. & Sharifi, R. 2009. Resistor type superconducting fault current limiter: Optimum shunt resistance determination to enhance power system transient stability. *IEEJ Transactions on Power and Energy*, 129(2): 299–308.

Hoshino, T., Salim, K.M., Kawasaki, A., Muta, I., Nakamura, T. & Yamada, M. 2003. Design of 6.6 kV, 100 A saturated DC reactor type superconducting fault current limiter. *IEEE Transactions on Applied Superconductivity*, 13(2 II): 2012–2015.

Kim, Y.P. & Ko, S.C. 2021. Dc current limiting characteristics of flux-coupled type sfcl using superconducting element connected in parallel in a dc system. *Energies*, 14(4).

Liu, X., Li, C., Shahidehpour, M., Gao, Y., Zhou, B., Zhang, Y., Yi, J. & Cao, Y. 2019. Fault current hierarchical limitation strategy for fault ride-through scheme of microgrid. *IEEE Transactions on Smart Grid*, 10(6): 6566–6579.

Manditereza, P.T. 2019. Fault Analysis. *Power System Protection in Smart Grid Environment*: 33–79.

Masaud, T.M. & Mistry, R.D. 2017. Fault current contribution of Renewable Distributed Generation: An overview and key issues. *2016 IEEE Conference on Technologies for Sustainability, SusTech 2016*: 229–234.

Matsumura, T., Kimura, A., Shimizu, H., Yokomizu, Y. & Goto, M. 2003. Fundamental performance of flux-lock type fault current limiter with two air-core coils. *IEEE Transactions on Applied Superconductivity*, 13(2 II): 2024–2027.

Meisen, P. 2014. Solar Electric and Solar Thermal Energy : A Summary of Current Technologies Table of Contents. , (619): 1–40.

Mohseni, A., Mohajer Yami, S. & Shayegani Akmal, A.A. 2011. Modeling of matrix fault current limiter and its verification. *2011 IEEE Electrical Power and Energy Conference, EPEC 2011*: 474–478.

Mutambudzi, R. & Raji, A.K. 2020. Impact of Distributed Generation on the Electric Protection System. *SSRN Electronic Journal*, (July).

Nemdili, S. & Belkhiat, S. 2012. Modeling and simulation of resistive superconducting fault-current limiters. *Journal of Superconductivity and Novel Magnetism*, 25(7): 2351–2356.

Noe, P.M. 2017. Superconducting Fault Current Limiters Table of Contents Motivation Basic Principles Design Example State-of-the-Art Summary Your questions are welcome any time.

Office of Electricity Delivery and Energy Reliability. 2009. Superconducting and Power Equipment. www.oe.energy.gov.

Patil, S. & Thorat, A. 2017. Development of fault current limiters: A review. *2017 International Conference on Data Management, Analytics and Innovation, ICDMAI 2017*: 122–126.

Razzaghi, R. & Niayesh, K. 2011. Current limiting reactor allocation in distribution networks in presence of distributed generation. *2011 10th International Conference on Environment and Electrical Engineering, EEEIC.EU 2011 - Conference Proceedings*: 1–4.

Safaei, A., Zolfaghari, M., Gilvanejad, M. & B. Gharehpetian, G. 2020a. A survey on fault current limiters: Development and technical aspects. *International Journal of Electrical Power and Energy Systems*, 118(November 2019): 105729. https://doi.org/10.1016/j.ijepes.2019.105729.

Safaei, A., Zolfaghari, M., Gilvanejad, M. & B. Gharehpetian, G. 2020b. A survey on fault current limiters: Development and technical aspects. *International Journal of Electrical Power and Energy Systems*, 118(November 2019).

Salam, I.U., Yousif, M., Numan, M., Zeb, K. & Billah, M. 2023. Optimizing Distributed Generation Placement and Sizing in Distribution Systems: A Multi-Objective Analysis of Power Losses, Reliability, and Operational Constraints. *Energies*, 16(16).

Shafiee, M.R., Shahbabaei Kartijkolaie, H., Firouzi, M., Mobayen, S. & Fekih, A. 2020. A dynamic multi-cell fcl to improve the fault ride through capability of dfig-based wind farms. *Energies*, 13(22): 1–14.

Sohail, I., Hussain, B., Abubakar, M., Sajjad, I.A., Nadeem, M.F. & Sarwar, M. 2022. SC Currents Minimization in Distributed Generation Embedded Distribution Networks with Optimal Application of FCLs. *CSEE Journal of Power and Energy Systems*, 8(5): 1388–1397.

Sule, A.H. 2022. Impact of Integration of Renewable Energy Sources on Power System Stability, Fault Protection and Location: A Review. *Direct Research Journal of Engineering and Information Technology*, 9(4): 87–100. http://directresearchpublisher.org/drjeit/.

Takele, H. 2022. Distributed generation adverse impact on the distribution networks protection and its mitigation. *Heliyon*, 8(6): e09624. https://doi.org/10.1016/j.heliyon.2022.e09624.

Tambunan, H.B., Aditya Pramana, P.A., Brian, B.B., Kusuma, A.A., Priambodo, N.W. & Munir, B.S. 2019. Multicriteria decision approach for selection of fault current limiters technology. *2019 Asia Pacific Conference on Research in Industrial and Systems Engineering, APCoRISE 2019*, 6: 3–7.

Wan, W., Zhang, P., Bragin, M.A. & Luh, P.B. 2022. Cooperative fault management for resilient integration of renewable energy. *Electric Power Systems Research*, 211(February): 108147. https://doi.org/10.1016/j.epsr.2022.108147.

Wang, R., Liao, M., Duan, X., Xie, D., Feng, Z. & Han, X. 2023. Development and parameters optimization of a self-driving fault current limiter. *Electric Power Systems Research*, 218(February): 109187. https://doi.org/10.1016/j.epsr.2023.109187.

Zhang, X. 2017. Resistive-type Superconducting Fault Current Limiter (RSFCL) and Its Application in Power Systems. , (August): 1–187.